Intel® Model: 18265NGW

FCC ID: PD918265NG

Intel® Model 18265NGW Embedded Inside a notebook brand Dell Model T17G WiGig Subsystem with RFEM 3

RF Exposure Power Density Evaluation and Test Report

July 2017

Revision 1.0

Intel

Notice:

All information provided here is subject to change without notice. Contact your Intel representative to obtain the latest Intel product specifications and roadmaps.

Intel technologies' features and benefits depend on system configuration and may require enabled hardware, software or service activation. Performance varies depending on system configuration. No computer system can be absolutely secure. Check with your system manufacturer or retailer or learn more at [intel.com].

Intel technologies may require enabled hardware, specific software, or services activation. Check with your system manufacturer or retailer.

You may not use or facilitate the use of this document in connection with any infringement or other legal analysis concerning Intel products described herein. You agree to grant Intel a non-exclusive, royalty-free license to any patent claim thereafter drafted which includes subject matter disclosed herein.

No license (express or implied, by estoppel or otherwise) to any intellectual property rights is granted by this document.

The products described may contain design defects or errors known as errata which may cause the product to deviate from published specifications. Current characterized errata are available on request.

Tests document performance of components on a particular test, in specific systems. Differences in hardware, software, or configuration will affect actual performance. Consult other sources of information to evaluate performance as you consider your purchase. For more complete information about performance and benchmark results, visit www.intel.com/benchmarks.

Copies of documents which have an order number and are referenced in this document may be obtained by calling 1-800-548-4725 or visit www.intel.com/design/literature.htm.

Intel, the Intel logo, {List of Intel trademarks} are trademarks of Intel Corporation or its subsidiaries in the U.S. and/or other countries.

*Other names and brands may be claimed as the property of others.

Contents

List of Figures

List of Tables

List of Abbreviations

Abbreviation	Definition
Ant	Antenna
Az	Azimuth
BB	Base Band
BF	Beam Forming
BT	Bluetooth
BW	Bandwidth
CPU	Central Processing Unit
El	Elevation
EM	Electro-Magnetic
GHz	Gigahertz
IF	Intermediate Frequency
MAC	Media Access Control
M.2	M2: Formerly known as Next Generation Form Factor (NGFF); used as specification for connectors of the expansion cards mounted on computer
mmWave	Millimeter Wave
PC	Personal Computer
PCIe	Peripheral Component Interconnect Express; a PCI Special Interest Group standard
R&D	Research and Development
RF	Radio Frequency
RFEM 3	Third-generation Radio Front End Module
RFIC	Radio Frequency Integrated Circuit
RX	Receive
SKU	Stock Keeping Unit, specific product model version
SoC	System-on-Chip
TDM	Time Division Multiplexing
TPC	Transmit Power Control
T/R SW	Transmit/Receive Switch
TX	Transmit

Abbreviation	Definition
WiGig	Wireless Gigabit Alliance – the alliance that promoted the 60GHz into 802.11ad standard.

1 Document Scope

1.1 Introduction

This report is submitted to support the compliance with the FCC rule located in Title 47 of the Code of Federal Regulations (CFR), parts §2.1093 and §15.255(g), of Intel 18265NGW WiGig module (FCC ID: PD918265NG), including an active antenna array, embedded inside the Dell model T17G.

Per the location of the active antenna array (a.k.a. RFEM 3) in the Dell model T17G platform, the distance between the antenna arrays to the body of an end user, at the closest contact point, will be in the near field.

In order to prove that during typical use the energy goes in most cases away from the human body, several tests of beamforming behavior was performed under different use cases conditions. The results are presented in this document.

These tests are supported by a determination of the near-field power average density performed using an EM simulation validated by a near field measurement. An EM simulation that includes the RFEM 3 transmitter model embedded inside the Dell model T17G is used to determine the worst case configuration and the correspondent near field power density. This worst case power density which is a conservative case considering that the energy is always oriented toward the human body is also validated by a near field measurement. The simulation method, the simulation results, and the near field measurement results are described in this document. The near field measurement system details are described in document [2]

Chapter 2 provides relevant background on Intel 18265NGW module. Chapter 3 shows the results of the beamforming behavior in operational mode directing the energy away from body. Appendix A describes the simulation methodology to determine the worst case configuration and the power density simulation results, and Appendix B shows the near field measurement results.

1.2 Associated Documents

Please note that this document covers non-confidential parts information; relevant details and explanations that qualify for confidentiality are included separately in the operational description and near-field measurements documents called references [1] and [2] therefore are not included in this report. However, some places in this document make cross-reference to the confidential reports for details about device operation and measurement principle.

[1] "Dell T17G – Theory of Operation Report Revision 1.0".

[2] "170108-01.TR02 - Dell T17G NF-Measurement_TR".

2 Background – WiGig System Operation

2.1 System Block Diagram

The Intel 18265NGW module is a solution for WiGig connectivity for various platforms. The Intel 18265NGW module can be embedded in a conventional clamshell PC as well as in modern 2-in-1 (detachable) platforms and tablet-like platforms (such as the Dell model T17G).

The client solution for Dell T17G includes the 18265NGW WiGig module (FCC ID: PD918265NG) connected to a beam forming antenna array RFEM 3 using one IF coaxial cable.

The WiGig module (FCC ID: PD918265NG) is a PCIe M.2 module consisting of a WiGig BB chip, which implements the WiGig MAC, Modem, BF algorithm, and active antenna array module control, as well as the BB + IF stage circuitry. Intel calls this module Oak Peak. (Note that Oak Peak uses the same WiGig base band silicon as Maple Peak.)

RFEM 3 (10101RRFW) is an active antenna array module, which converts the IF signal to a 60 GHz signal. It also performs the beam forming functionality by phase[1] shifting the RF signal that goes to each antenna. The RFEM 3 is slave to the WiGig BB chip, since all module control and algorithms run on the BB chip.

Intel System-on-Chip (SoC) houses the central processing unit (CPU), which executes applications and provides command and control of the client solution, including all I/O data and addressing.

---

[1] *Each antenna is excited by an amplitude at a defined phase angle. RFEM 3 feeding circuit has 2 bit phase shifter. Therefore, the phase's values can be 0, 90, 180, or 270 degrees.*
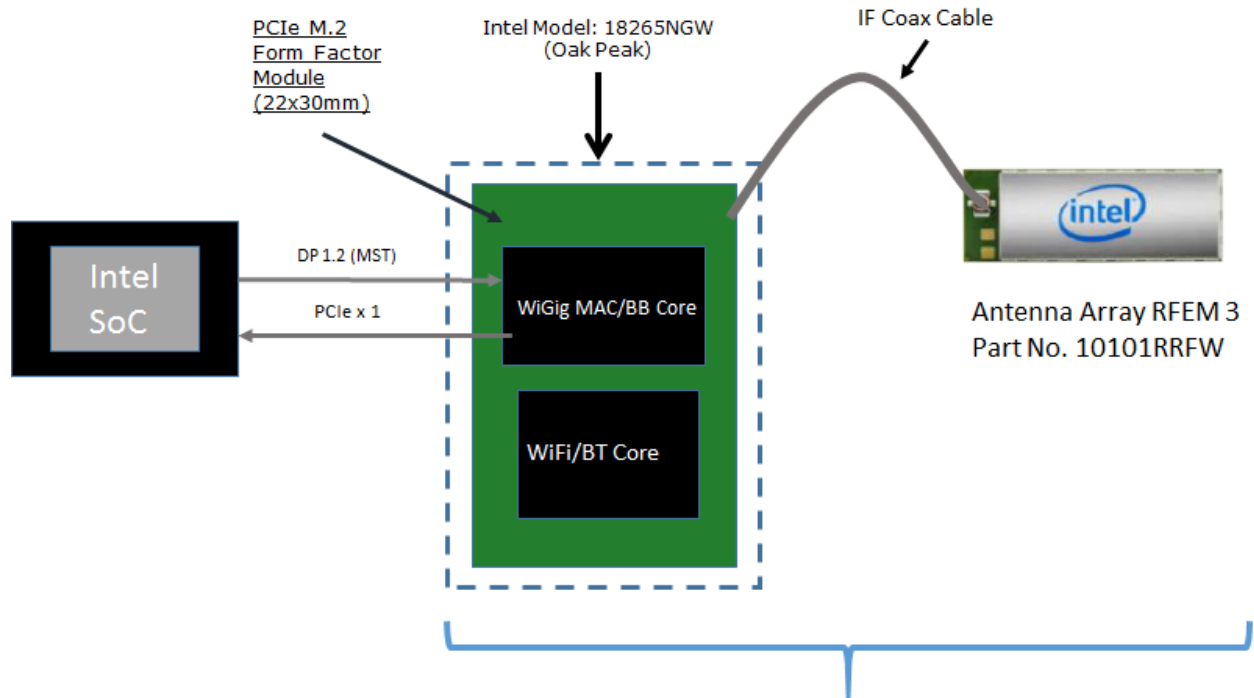
Figure 1 – Intel 18265NGW module system block diagram

Note: Also known by Intel internal project code name "Oak Peak," the above-described WiGig module solution still uses the "Maple Peak" Intel chipset (both MAC/BB chip and radio chip).

2.2 Beamforming

Achieving high-bandwidth communication over 60 GHz channels usually requires directional antennas at the transmitter and receiver sides. In consumer electronics, fixed directional or mechanically-rotated antennas are not practical, and electronically steerable antennas are usually used.

In the Intel 18265NGW module, an electronically-steerable antenna array is used. Beam forming protocol (defined in the IEEE 802.11ad standard) is used to find the right direction for setting both the RX and TX antenna directions.

Due to the RFEM structure, it is not easy to predict the direction and beam forming combination that yields the maximum energy in near field. To find this value, a search over the possible beam forming combination was made and the worst case value was taken. A detailed explanation of this process can be found in Section A.1.4.

2.3 TX Duty Cycle

The WiGig protocol, as defined in ISO/IEC/IEEE 8802-11:2012/Amd.3:2014(E), Clause 21, is packet-based, with time division multiplexing (TDM). The Intel 18265NGW module is configured to guarantee that the TX-Duty-Cycle, defined as the ratio of the duration of all transmissions to the total time, is at most 70% over any 10-second period. This was established by worst-case analysis, as derived from full-system simulation, and verified by measurements.

The limited TX-Duty-Cycle is established based on HW and FW implementation with a measurement duration of ~100 ms (102.4 ms) and 10-second averaging; other details are provided in reference [1]. The 70% duty cycle limitation is guaranteed, independent of user activity, and therefore adheres to the source-based time-averaging definition in Title 47 of the Code of Federal Regulations (CFR) 2.1093(d)(5).

In addition, measurements of the Intel 18265NGW module, configured to obtain maximal TX-Duty-Cycle in a fully loaded system, resulted in an actual maximum TX-Duty-Cycle of 58% over any 10-second period, lower than the upper bound derived from the analysis in this section.

2.4 Intel 18265NGW module in Dell model T17G

Intel produces several HW SKUs (variations) of the Intel 18265NGW module, which target different types of customer platform products.

Dell uses the Intel 18265NGW module inside the Dell model T17G platform. This SKU is characterized by

1. Supporting channels **1+2+3**

2. Reduced power emission, which translates to
   a. Maximum transmit conducted power of **1.5 dBm** aggregated conducted power at the antenna ports.
   b. Maximum TX duty-cycle of **70%**.

3 Beamforming Behavior in Operational Mode

3.1 Introduction

The goal of this section is to show that during typical use of RFEM 3 inside Dell Model T17G, the energy would go away from the human body. This will be showed by performing several beamforming behaviour tests taking into account different typical height / distances.

3.2 Environmental Conditions

At the site where the measurements were performed the following limits were not exceeded during the tests:

Temperature	24ºC ± 1ºC
Humidity	55% ± 10%

3.3 Test samples

Sample	Control #	Description	Model	Serial #	Date of receipt
#01	170108-01.S05	Wireless Module installed in tablet	18265NGW inside T17G	4314099600001	2017-03-06
	170108-01.S06	AC Adapter	NA	NA	2017-03-06
#02	170228-01.S14	Dock Station	WIDOCK-SDS	EZWI51100184	2017-05-11
	170228-01.S14	AC Adapter	NA	NA	2017-05-11

3.4 EUT Features

Brand Name	Intel Model 18265 inside Dell Model T17G
Model Name	Client Platform Design Guidelines
FCC/IC ID	FCC ID: PD918265NGW/IC ID: 1000M-18265NG
Software Version	3.0.41131.1
Prototype / Production	Production
Host Identification	Intel
Exposure Conditions	Body worn – localized free space power density
Supported Radios	WiGig 60GHz (57.24 – 63.72 GHz) 802.11b/g/n 2.4GHz (2400.0 – 2483.5 MHz) 802.11a/n/ac 5.2GHz (5150.0 – 5250.0 MHz) 5.3GHz (5250.0 – 5350.0 MHz) 5.6GHz (5470.0 – 5725.0 MHz) 5.8GHz (5725.0 – 5825.0 MHz) Bluetooth 2.4GHz (2400.0 – 2483.5 MHz)
Antenna Information	RFEM3 (10101RRFW)

3.5 Test System Description

3.5.1 Measurement setup

- The dock station is placed on the table with a height of 80 cm above the horizontal ground plane.

- The person is holding the EUT horizontally on his lap.

- Initially, the EUT is touching the person's lap at the evaluation plane as shown in Figure 2. In this case, the dock station and the EUT are at the same height i.e. 80 cm above the horizontal ground plane.
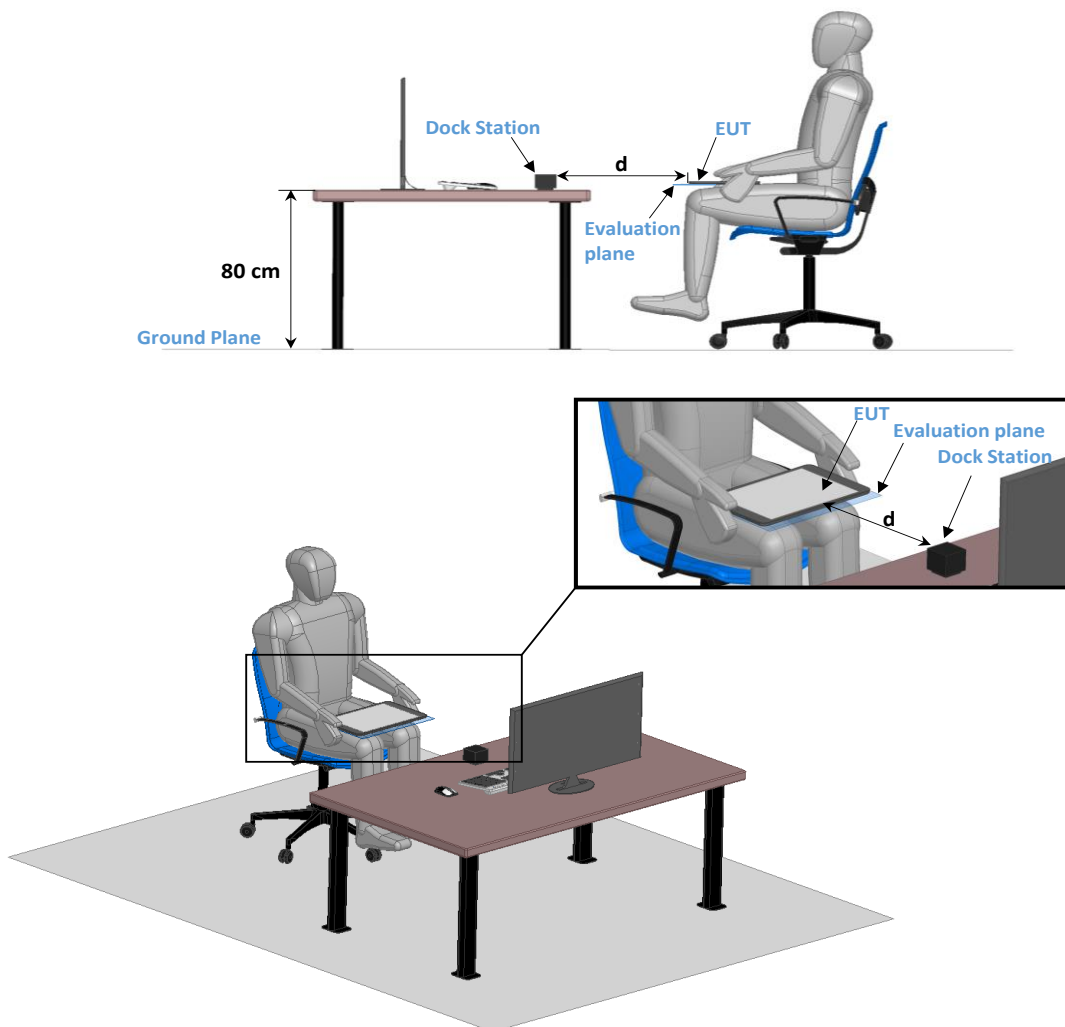
Figure 2– Qualitative measurement test setup

3.5.2   Test configuration

- The EUT and the dock station are set in operation mode and a link condition between the two samples is made using a link software (Wireless Dock Manager, Version 3.0.41131.1)

- The measurement is performed at several distances (d) between the dock station and the EUT i.e. 30 cm, 60 cm, 120 cm. These distances represent three typical use cases and describe three different beam coverages for the operational subsets

- For each distance (d) the test is performed for several heights (h) between the EUT exposure's plane and the person's lap. The height is modified (Figure 4) as described below

  (1) The EUT is raised from the lap position (h=0) until a transition height (h=h_t) where a handover between subsets is observed.

  (2) The EUT height is increased until it has passed the transition region.

  (3) The EUT is moved back toward the lap in reverse order until it has passed the lower boundary of the transition region.

- Styrofoam spacers with specific heights are used between the EUT and the person lap's (Figure 3)

- Beam forming triggering in operational mode: when the link is not in maximum MCS (MCS 12) the SW triggers beam forming each 4 seconds. When there is abrupt MCS degradation (3 MCS steps) compared to the chosen MCS, or no response from the other side, then there is immediate beam forming triggering. For each EUT position, the measurement time is selected to be sufficient for conditions to stabilize and to record the beamforming code instances.
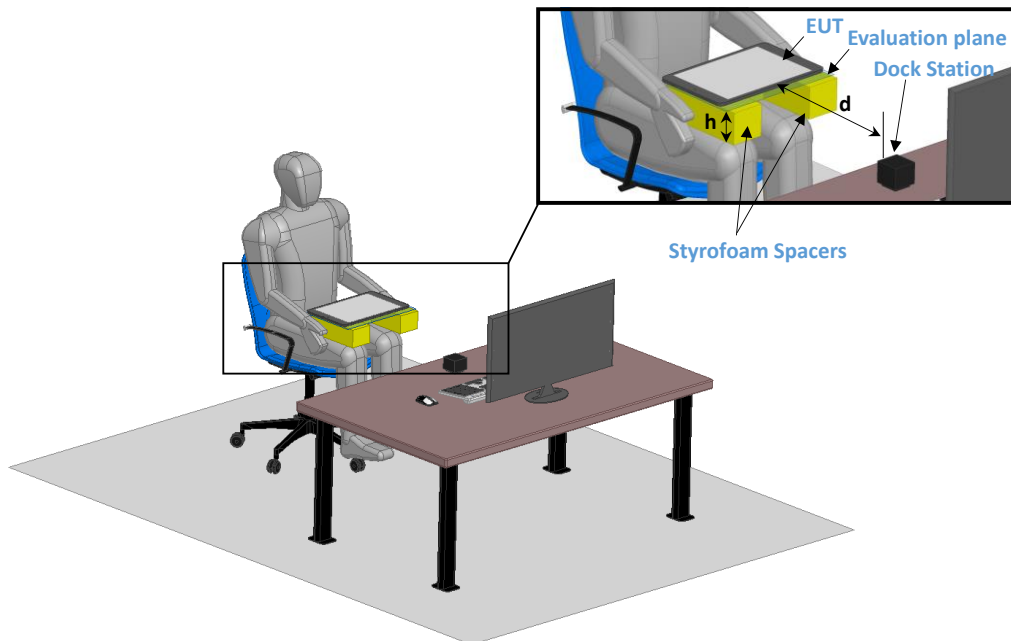
Figure 3– Qualitative measurement test configuration
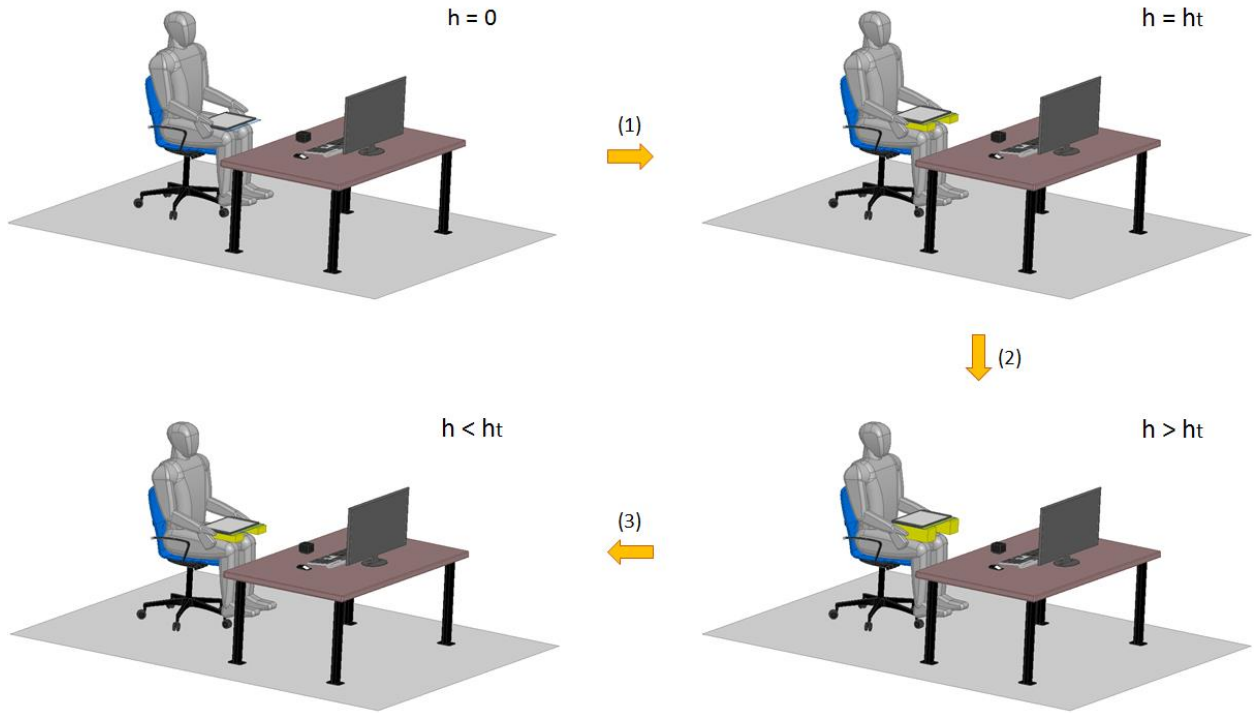
Figure 4– Height variation for transition zone determination

Table 2 summarizes the realized test configuration

Table 2 – Test configuration summary

Test number	EUT to dock station distance (d)	EUT to person laps distance (h)
1	30 cm	0, 2, 4, 6, 8 and 10 cm
2	60 cm	0, 2, 4, 6, 8, 10, 12 and 14 cm
3	120 cm	0, 2, 4, 6, 8, 10, 12, 14, 16,18 and 20 cm

3.5.3   Results types

In this paragraph, we present the types of results that will be obtained in the tests defined in the previous section.

3.5.3.1   Subset and beamforming code selection

As mentioned in the introduction, the goal of this measurement is to prove that energy goes away from the body when the EUT is at its proximity. The metric that can show this behaviour is the percentage of operation of each subset.

Indeed, Figure 5 illustrates the position of the RFEM 3 antenna when the EUT is placed horizontally; this is the case of all test configurations defined in Table 2. The same figure shows the nominal beam direction of each subset. In this case, the tests should prove that subset 2 is operational in the majority of time when the DUT is close to the body in order to direct the beam away.
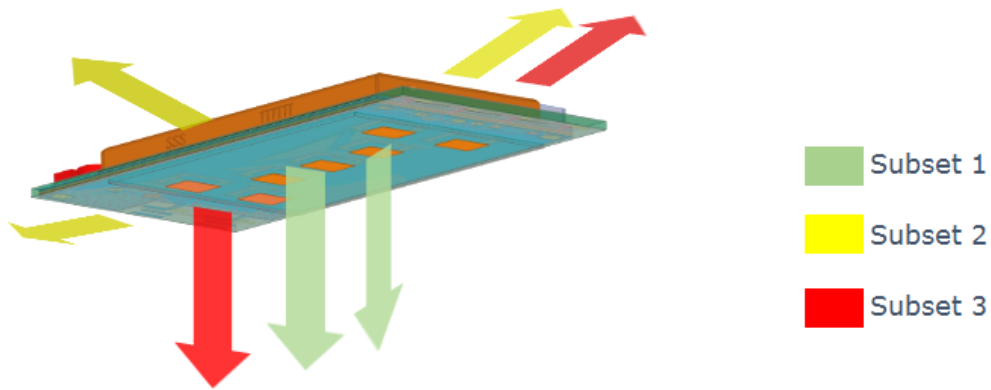
- Subset 2 directed away from leg
- Subset 1 and Subset 3 directed towards leg

Figure 5– RFEM 3 Subsets nominal beam directions

Note that when a subset is operational, a beamforming code (phases' combination of the subset's elements) among a set of codes (instances) for each subset is realized.

Table 3 illustrate the sectors numbers associated to each subset. A sector related to a subset is a phase's combination of this subset elements.

Table 3 – Subsets' sectors

Number of Sector															
1	2	3	4	5	6	7	8	9	10	11	12	13	14	15	16
17	18	19	20	21	22	23	24	25	26	27	28	29	30	31	32
33	34	35	36	37	38	39	40	41	42	43	44	45	46	47	48
49	50	51	52	53	54	55	56	57	58	59	60	61	62		

Subset 1   Subset 2   Subset 3

3.5.3.2 Transition zone determination

The second parameter to be studied in these tests is the existence of a transition zone in which a handover from subset to another is observed. This is essential to prove the efficiency of the beamforming algorithm.

3.5.4 Test results

Figure 6, Figure 7 and Figure 8 shows the test results of the subset operation according to the EUT to lap distance (h), for the three horizontal distances: 30, 60, and 120 cm respectively. The x-axis represents the height above lap while the y-axis represents, for each subset, the percentage of subset operation.

1. **Test 1 results at 30 cm distance**
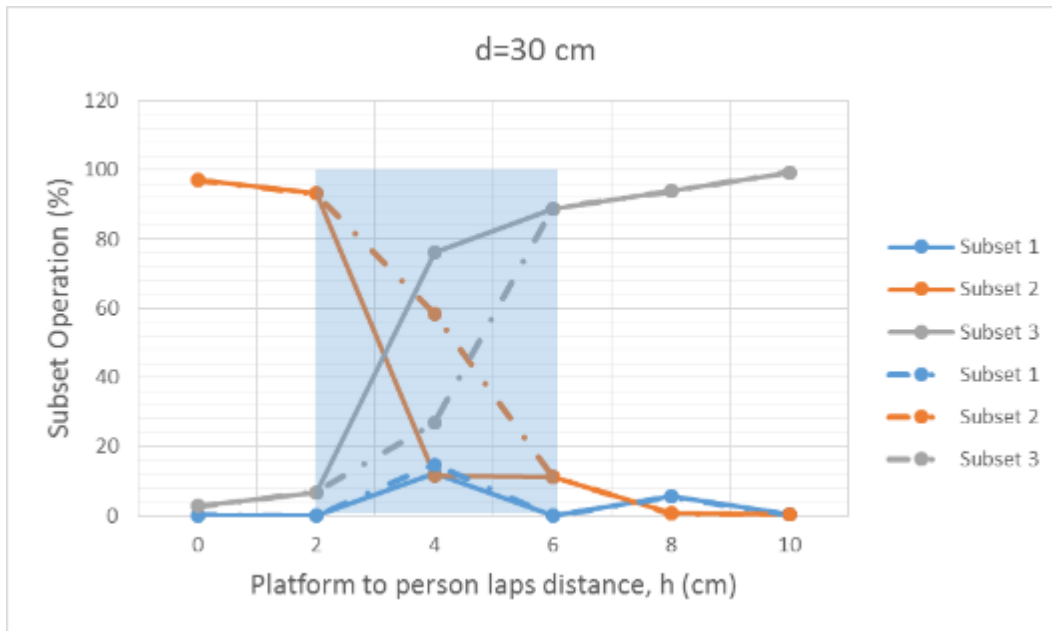
Figure 6– Percentage of subset operation at d=30cm

2. Test 2 results at 60 cm distance
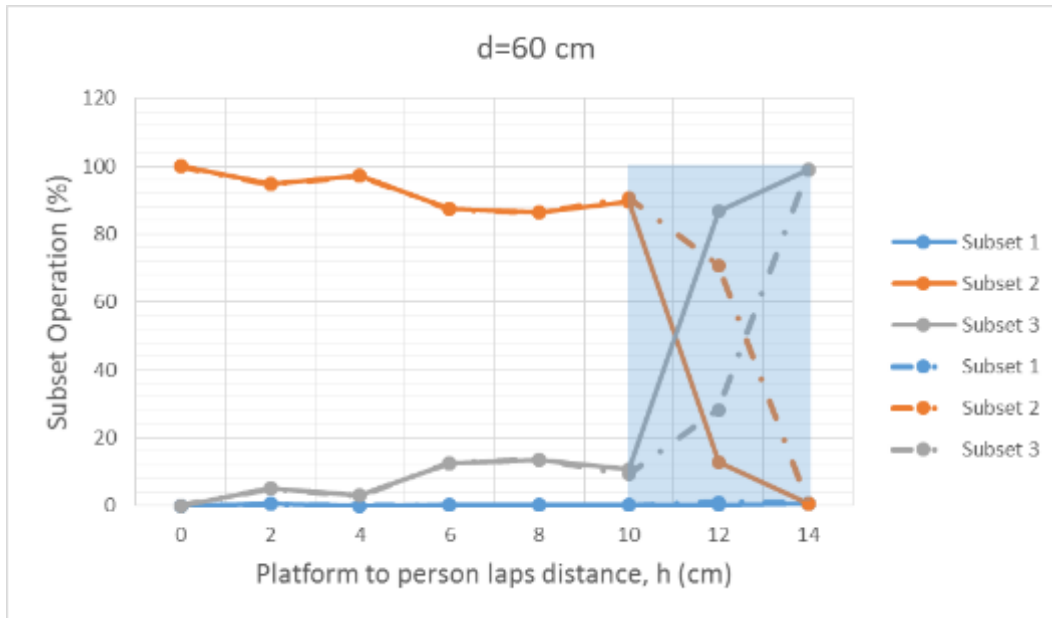
Figure 7– Percentage of subset operation at d=60cm

3. Test 3 results at 120 cm distance
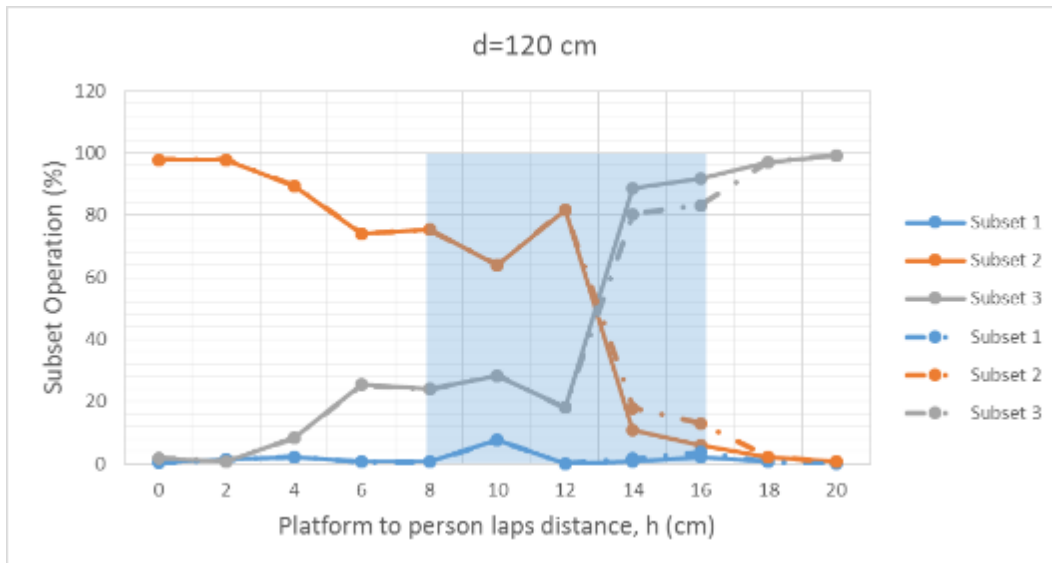
Figure 8– Percentage of subset operation at d=120cm

3.5.5   Conclusion

The test results presented in the previous section show that, at each horizontal distance:

- When the EUT is placed close to the lap, subset 2 (orange line) with a beam directed away from the body is operational almost all the time.

- When the EUT is moved forward from the lap, a transition zone is observed (blue area) and a handover from subset 2 to subset 3 is done after this transition zone

- When the EUT is moved back toward the lap in reverse order, the transition zone is observed again and a switch from subset 3 to subset 2 is observed starting from the lower boundary of the transition zone.

When the horizontal distance increases, the transition height is observed at higher distance between the EUT and the lap.

These test results confirm that the beam steering algorithm behaves in such a manner as to direct the energy away from the body while maintaining a good link budget.

4 Compliance Assessment

The goal of the tests presented in the previous sections is to determine the likelihood that energy would go towards or away from the human body during typical use.

It was demonstrated that in the vast majority of the cases, over typical usage/height/distances, the chosen subset directs energy away from the body.

As further supplemental compliance supporting information, numerical simulation results in Appendix A validated by near-field measurement results in Appendix B show that worst case power density is below the RF exposure FCC limit.

In Appendix A, we will present a worst case scenario defined using simulation, and validated by measurement in Appendix B. This case is "conservative" considering that the energy is always oriented toward the human body, which will be rarely observed in typical use as shown in Section 3.

Table 4 shows the simulated maximum spatially averaged power density, over $1cm^2$ in the evaluation plane of the Intel 18265NGW module, embedded in the Dell model T17G.

Table 4 – Summary of simulation results for RF exposure compliance

Parameter	Value
Total conducted power	1.5 dBm
Maximum spatially averaged power density, over $1cm^2$ - Simulation at 100% Duty Cycle	0.907 mW/cm^2
Maximum TX duty-cycle	70%
Maximum spatially averaged power density, over $1cm^2$ - Simulation at 70% Duty Cycle	**0.635 mW/cm²**

Therefore, with 0.635 mW/cm^2 spatially averaged power density value, Intel 18265NGW module, embedded in Dell model T17G, complies with FCC rule located in Title 47 of the Code of Federal Regulations (CFR) parts §2.1093 and §15.255(g).

The simulation results are validated by near field measurement using a near field probe. Because measurement results are unavailable at distances closer than 2 mm by probe limitation, the comparison between simulation and measurement is performed at 2 mm and 5 mm from the evaluation plane. The results are presented Appendix B.

Appendix A: Supplemental Numerical Modeling for RF Exposure Power Density Evaluation

A.1 Platform Simulation Methodology

A.1.1   Assessment considerations

During the system operation mode, it is challenging to define a practical system worst-case scenario in which the user is exposed to the highest emission level. To ensure coverage of the highest emission, the analysis of the worst-case corner condition is used and is emphasized in the following:

1. Platform orientation with respect to human body – In most of the cases, when the platform is very close to the human body, and the energy is directed to the human body, the human body will attenuate the signal. In this case, a reliable link can't be achieved. When a reliable link can't be maintained, the system enters search mode. In search mode, the system will transmit a low-duty cycle of less than 1%. This search mode contains signals which happen every 100ms at the maximum output power. However, in the analysis done for this document, the system is simulated in operational mode (not in search mode), operating at 70% duty cycle, which is much higher than the search mode.

2. Energy direction, beam forming – In order to avoid human body attenuation or object blockage of a reliable link, the system beam forming will automatically search for a path that will establish a more reliable link. So, in real life, in most of the cases the EM path will not be directed towards the human body (see Section 3). However, in the analysis presented in this document, worst-case beam forming direction is used.

Please note that the above worst-case assessment description is very conservative in that it is very unlikely that this case would happen under normal usage conditions. Since we cannot state with 100% certainty that this is impossible, we kept this worst-case assessment methodology for supplemental purposes. We ask that this be taken into consideration.

A.1.2   Near field and transition-zone field results

Finding the worst-case emission in the near field across the platform boundary requires searching on two orthogonal domains. One domain is the location – the need to find the place that has the worst-case energy. The other domain that has to be searched is the range of antenna phases – the need to search over the various antenna phases and find the antenna phase combination that gives the worst-case value. Section A.1.4 explains how these two worst-case (location and phase) searches are investigated.

After the completion of the worst-case phase analysis, the phases found during this analysis are used to find the worst-case spatially averaged power density across a 1cm^2, for RF exposure evaluation purposes. EM simulation is used for this analysis.

Near-field analysis is simulated and correlated against measured lab results.

A.1.3 Simulation tool

A.1.3.1 Tool description

For the EM simulation, the commercially-available ANSYS Electronics Desktop 2016 (HFSS) is used. The ANSYS HFSS tool is used in the industry for simulating 3D, full-wave electromagnetic fields. Intel uses this EM simulation tool due to its gold-standard accuracy, advanced solver, and high-performance computing technology capabilities for doing accurate and rapid design of high-frequency components.

A.1.3.2 Solver description

The HFSS simulation is performed using the Finite Element Method, which operates in the frequency domain. The HFSS is based on an accurate direct solver with first order basis functions.

A.1.3.3 Convergence criteria and power density calculations

The HFSS uses a volume air box containing the simulated area to calculate the EM fields. The box is truncated by a Perfect Match Layer (PML) boundary condition. The simulation uses the adaptive mesh technique (see Figure 9) meet the exit criteria of delta S < 0.02. The delta S is the change in the magnitude of the S-parameters between two consecutive passes; if the magnitude and phase of all S-parameters change by an amount less than the Maximum-Delta-S-per-Pass value from one iteration to the next, the adaptive analysis stops.

Unit: mm
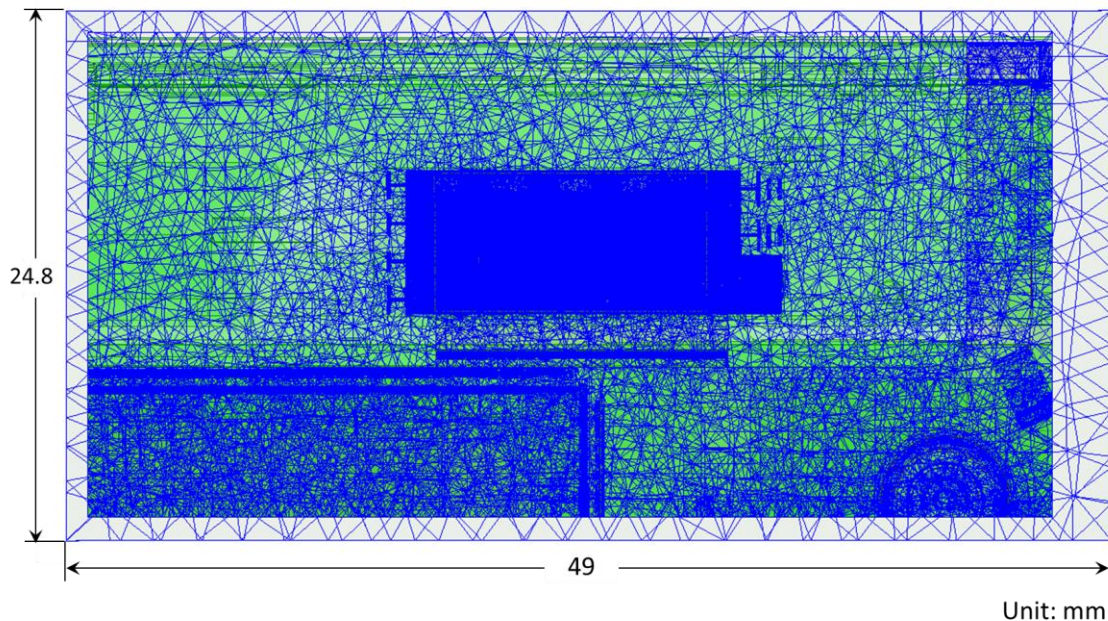
Figure 9 – Illustration of the adaptive mesh technique

After having the simulated electrical and magnetic (E and H) fields at each point in the mesh, the Poynting vector is calculated. The spatially averaged power density on a given surface is calculated as the surface integral of the Poynting vector:

$$W = \frac{1}{2}\text{Re} \int_S (\vec{E} \times \vec{H}^*) \cdot \vec{n} dS$$

Notes:

1. HFSS phasors in the field calculator are peak phasors, which leads to the ½ factor in the Poynting vector calculation.

2. Figure 9 is an illustration of the adaptive mesh technique and is presented in the context of simulation methodology presentation.

A.1.4 Finding the near-field, worst-case simulation configuration

As explained previously, near-field analysis requires finding the worst-case location (along the searched plane) and antenna phase values. As further explained, the search should be done on two domains:

1) Look for the worst-case position (across the search plane).

2) Look for the two worst-cases antenna phases.

Note: The search planes are defined as the planes used for the calculation of the two worst-cases antenna phase combinations. The new RFEM 3 antenna is intended to operate according to one of three predefined subsets[2]. For each subset an evaluation plane is defined taking into account the radiation direction of this subset. For subset 1 and 3 the evaluation plane corresponds to the tablet back–side exposure. For subset 2 the evaluation plane corresponds to the tablet front-edge exposure. The two domains described in 1) and 2) are applied for each subset separately in its evaluation plane in order to find worst case power density.
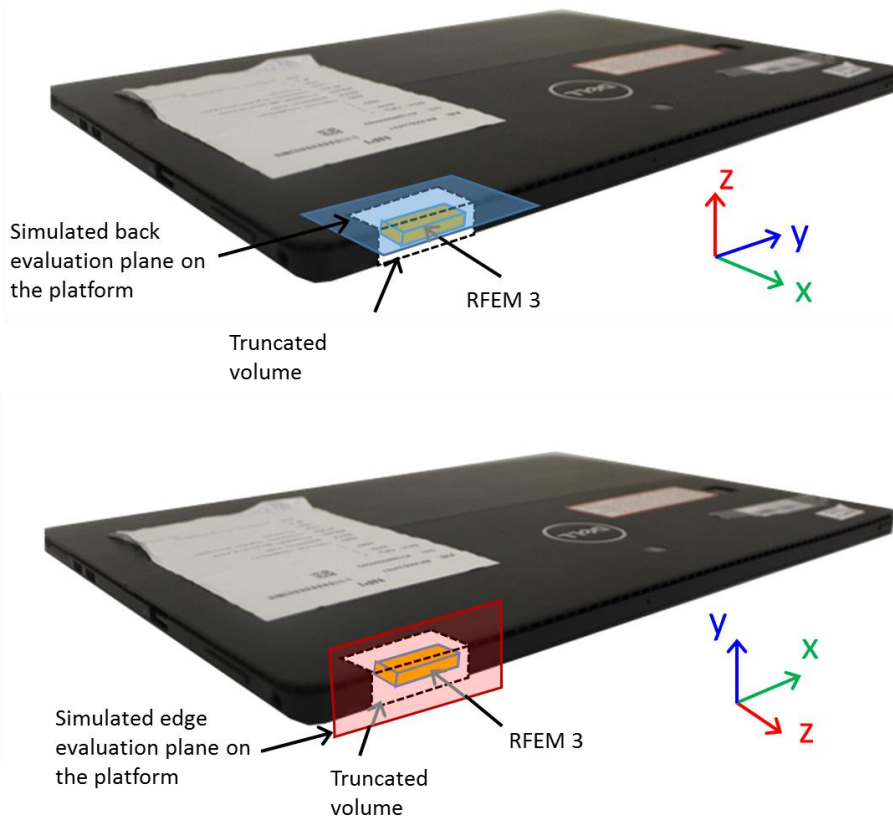
Figure 10 – The x-y search on the back evaluation plane (blue area) and edge evaluation plane (red area)

---

[2] *A subset is a group of radiating elements which are excited simultaneously with the same amplitude. In RFEM 3, the number of subsets is three.*

Note that for the xyz coordinate references used throughout this report, we always consider the z-axis as being towards the body direction. This consideration is used to conserve a general consistency for the field's representation and calculations in the worst-case determination procedure detailed below. In summary, the xy plane is the evaluation plane, and the z-axis is the vector in propagation direction towards the body.

A.1.4.1 Terminology

- Element – Each one of the radiating elements that are used in the system. We denote the antenna element with index **k** in this explanation.
- N – Number of chains (RFEM 3 includes 24 radiated antenna elements – **N**=24). As described in the previous section, there are three subsets in RFEM 3. These subsets, named subset 1, subset 2 and subset 3, are composed of 10, 11 and 11 active elements respectively. For each subset, a set of elements from the 24 radiating antennas is activated).
- Point – Each point on the grid that is used for searching for the worst- case position. They are spaced 0.1mm from each other. The grid point would be denoted as **g** in this explanation.
- Complex E field vector generated by the kth antenna element at point g:

$$\overrightarrow{E_{k,g}} = \vec{x}\left(\text{Re}[E_{kx,g}] + j\text{Im}[E_{kx,g}]\right) + \vec{y}\left(\text{Re}[E_{ky,g}] + j\text{Im}[E_{ky,g}]\right) + \vec{z}\left(\text{Re}[E_{kz,g}] + j\text{Im}[E_{kz,g}]\right)$$

- Complex H field vector generated by the kth antenna element at point g:

$$\overrightarrow{H_{k,g}} = \vec{x}\left(\text{Re}[H_{kx,g}] + j\text{Im}[H_{kx,g}]\right) + \vec{y}\left(\text{Re}[H_{ky,g}] + j\text{Im}[H_{ky,g}]\right) + \vec{z}\left(\text{Re}[H_{kz,g}] + j\text{Im}[H_{kz,g}]\right)$$

- $\hat{x}$, $\hat{y}$, $\hat{z}$ – unit direction vectors having unit magnitude and mutually orthogonal to each other.
- Without loss of generality in this explanation, RFEM 3 and the search plane are in the $\hat{x}$, $\hat{y}$ plane, and the integrated 1cm^2 plane is perpendicular to direction $\hat{z}$.
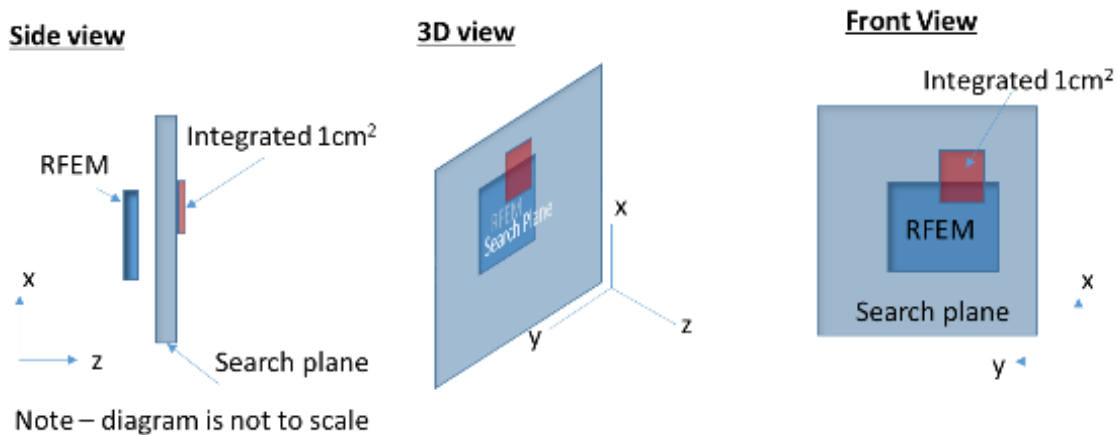

Figure 11 – Near field worst-case terminology and orientation

A.1.4.2 Primer on field vector representation

For each subset, *E* and *H* fields generated by the k chain are

$$\overrightarrow{E_k} = \vec{x}(\text{Re}[E_{kx}] + j\text{Im}[E_{kx}]) + \vec{y}\left(\text{Re}[E_{ky}] + j\text{Im}[E_{ky}]\right) + \vec{z}(\text{Re}[E_{kz}] + j\text{Im}[E_{kz}])$$

Intel

$$\overrightarrow{H_k} = \vec{x}(\text{Re}[H_{kx}] + j\text{Im}[H_{kx}]) + \vec{y}\big(\text{Re}[H_{ky}] + j\text{Im}[H_{ky}]\big) + \vec{z}(\text{Re}[H_{kz}] + j\text{Im}[H_{kz}])$$

For each subset, *E* and *H* fields generated by all *N* chains (only subset elements are activated) are

$$\overrightarrow{E_{\text{All}}} = \vec{x}\sum_{k=1}^{N}(\text{Re}[E_{kx}] + j\text{Im}[E_{kx}]) + \vec{y}\sum_{k=1}^{N}\big(\text{Re}[E_{ky}] + j\text{Im}[E_{ky}]\big) + \vec{z}\sum_{k=1}^{N}(\text{Re}[E_{kz}] + j\text{Im}[E_{kz}])$$

$$\overrightarrow{H_{\text{All}}} = \vec{x}\sum_{k=1}^{N}(\text{Re}[H_{kx}] + j\text{Im}[H_{kx}]) + \vec{y}\sum_{k=1}^{N}\big(\text{Re}[H_{ky}] + j\text{Im}[H_{ky}]\big) + \vec{z}\sum_{k=1}^{N}(\text{Re}[H_{kz}] + j\text{Im}[H_{kz}])$$

The Poynting vector generated by all *N* chains is

$$\overrightarrow{P_{\text{General,All}}} = \frac{1}{2}\overrightarrow{E_{\text{All}}} \times \overrightarrow{H_{\text{All}}^{*}}$$

$$= \frac{1}{2}\langle\vec{x}\left\{\sum_{k=1}^{N}\big(\text{Re}[E_{ky}] + j\text{Im}[E_{ky}]\big)\sum_{k=1}^{N}(\text{Re}[H_{kz}] - j\text{Im}[H_{kz}])\right.$$

$$\left. - \sum_{k=1}^{N}(\text{Re}[E_{kz}] + j\text{Im}[E_{kz}])\sum_{k=1}^{N}\big(\text{Re}[H_{ky}] - j\text{Im}[H_{ky}]\big)\right\}$$

$$+ \vec{y}\left\{\sum_{k=1}^{N}(\text{Re}[E_{kz}] + j\text{Im}[E_{kz}])\sum_{k=1}^{N}(\text{Re}[H_{kx}] - j\text{Im}[H_{kx}])\right.$$

$$\left. - \sum_{i=1}^{N}(\text{Re}[E_{kx}] + j\text{Im}[E_{kx}])\sum_{k=1}^{N}(\text{Re}[H_{kz}] - j\text{Im}[H_{kz}])\right\}$$

$$+ \vec{z}\left\{\sum_{k=1}^{N}(\text{Re}[E_{kx}] + j\text{Im}[E_{kx}])\sum_{k=1}^{N}\big(\text{Re}[H_{ky}] - j\text{Im}[H_{ky}]\big)\right.$$

$$\left. - \sum_{k=1}^{N}\big(\text{Re}[E_{ky}] + j\text{Im}[E_{ky}]\big)\sum_{k=1}^{N}(\text{Re}[H_{kx}] - j\text{Im}[H_{kx}])\right\}\rangle$$

Power flow is

$$
\begin{aligned}
\mathrm{Re}\!\left[\overrightarrow{P_{\mathrm{General,All}}}\right] = \frac{1}{2}\langle \vec{x} &\left\{ \sum_{k=1}^{N}\mathrm{Re}\!\left[E_{ky}\right]\sum_{k=1}^{N}\mathrm{Re}\!\left[H_{kz}\right] + \sum_{k=1}^{N}\mathrm{Im}\!\left[E_{ky}\right]\sum_{k=1}^{N}\mathrm{Im}\!\left[H_{kz}\right] - \sum_{k=1}^{N}\mathrm{Re}\!\left[E_{kz}\right]\sum_{k=1}^{N}\mathrm{Re}\!\left[H_{ky}\right] \right.\\
&\left. - \sum_{k=1}^{N}\mathrm{Im}\!\left[E_{kz}\right]\sum_{k=1}^{N}\mathrm{Im}\!\left[H_{ky}\right] \right\}\\
+ \vec{y} &\left\{ \sum_{k=1}^{N}\mathrm{Re}\!\left[E_{kz}\right]\sum_{k=1}^{N}\mathrm{Re}\!\left[H_{kx}\right] + \sum_{k=1}^{N}\mathrm{Im}\!\left[E_{kz}\right]\sum_{k=1}^{N}\mathrm{Im}\!\left[H_{kx}\right] - \sum_{k=1}^{N}\mathrm{Re}\!\left[E_{kx}\right]\sum_{k=1}^{N}\mathrm{Re}\!\left[H_{kz}\right] \right.\\
&\left. - \sum_{k=1}^{N}\mathrm{Im}\!\left[E_{kx}\right]\sum_{k=1}^{N}\mathrm{Im}\!\left[H_{kz}\right] \right\}\\
+ \vec{z} &\left\{ \sum_{k=1}^{N}\mathrm{Re}\!\left[E_{kx}\right]\sum_{k=1}^{N}\mathrm{Re}\!\left[H_{ky}\right] + \sum_{k=1}^{N}\mathrm{Im}\!\left[E_{kx}\right]\sum_{k=1}^{N}\mathrm{Im}\!\left[H_{ky}\right] - \sum_{k=1}^{N}\mathrm{Re}\!\left[E_{ky}\right]\sum_{k=1}^{N}\mathrm{Re}\!\left[H_{kx}\right] \right.\\
&\left. - \sum_{k=1}^{N}\mathrm{Im}\!\left[E_{ky}\right]\sum_{k=1}^{N}\mathrm{Im}\!\left[H_{kx}\right] \right\}\rangle
\end{aligned}
$$

A.1.4.3 Domain search for worst-case direction

The two domain search is completed (for each subset) as follows:

A. First find a direction (location) for the worst-case 1cm^2 square averaging area using upper-bound methods.

   The basic concept behind the upper-bound method is to assume that there could be an "ideal beam forming" mechanism that could align the phases of all the elements for both E and H fields. (Obviously, in real life this cannot happen. This is the reason that this is an upper-bound method). When this ideal mechanism is used, then all the complex phasors are aligned to the same phase, hence the phasor absolute value can be used instead of the phasor. The E (and H) field for any direction is the sum of the magnitude of the fields (look at item 3, below, for a more formal description).

   This method provides the worst-case position independent of the antenna phases. It allows finding the worst-case location with this "ideal beam forming" mechanism.

   Item 3, below, translates the above verbal description into more formal mathematical wording.

B. After the worst-case direction is found using the upper-bound method for each subset, the antenna phases are aligned to this direction. The antenna phases are aligned to maximize the power across the 1cm^2 averaging area that was found using the upper-bound method. The method that is used to find the required antenna phases is as follows: first order the antennas of the subset according to the power contribution on the found 1cm^2 from the highest to the lowest. Then start by activating the antenna that contributes the most, set its phase to 0, and then activate the 2nd antenna and search over the phases for the 2nd antenna. Choose the phase that maximizes the power of the two antenna elements. To find the phase for the third antenna, fix antenna 1's phase to zero and antenna 2's phase to the value that was found before. Then search for the phases for the third antenna that maximize the power. Continue with the same process until you reach the last subset

Intel

element. The same process is used to find the second worst case.

C. Calculate the power density with the antenna phases that were found in the previous item (item B).

The above process can be written as the following algorithm:
1. A grid is defined with 0.1mm spacing.
2. At each point in the grid, the complex E and H fields are calculated using each one of all radiating elements in the involved subset, separately. Each one of the calculated E and H fields are 3D complex vectors, so the simulation output from this stage is 10, 11, 11 3D complex E field strength vectors and 10, 11, 11 3D complex H field strength vectors for the three subsets respectively . The vectors are defined as:

$$\overrightarrow{E_{k,g}} = \vec{x}\left(\text{Re}[E_{kx,g}] + j\text{Im}[E_{kx,g}]\right) + \vec{y}\left(\text{Re}[E_{ky,g}] + j\text{Im}[E_{ky,g}]\right) + \vec{z}\left(\text{Re}[E_{kz,g}] + j\text{Im}[E_{kz,g}]\right) \text{ and}$$
$$\overrightarrow{H_{k,g}} = \vec{x}\left(\text{Re}[H_{kx,g}] + j\text{Im}[H_{kx,g}]\right) + \vec{y}\left(\text{Re}[H_{ky,g}] + j\text{Im}[H_{ky,g}]\right) + \vec{z}\left(\text{Re}[H_{kz,g}] + j\text{Im}[H_{kz,g}]\right)$$

3. Upper-bound assumption is used to derive the E and H field on each one of the grid points. The following items describe the upper-bound method that is used:
   a. The calculation is made separately for E field and H field.
   b. For E field, the following calculation is made independently for each one of the grid points:

$$\overrightarrow{E_{\text{UB},g}} = \vec{x}\sum_{k=1}^{N}\sqrt{\text{Re}[E_{kx,g}]^2 + \text{Im}[E_{kx,g}]^2} + \vec{y}\sum_{k=1}^{N}\sqrt{\text{Re}[E_{ky,g}]^2 + \text{Im}[E_{ky,g}]^2}$$
$$+ \vec{z}\sum_{k=1}^{N}\sqrt{\text{Re}[E_{kz,g}]^2 + \text{Im}[E_{kz,g}]^2} = \vec{x}\sum_{k=1}^{N}|E_{kx}| + \vec{y}\sum_{k=1}^{N}|E_{ky,g}| + \vec{z}\sum_{k=1}^{N}|E_{kz,g}|$$

   The magnitude of the complex E vector is summed over the antenna elements in a subset. The summation is done for each one of the grid points, and for each one of the elements in each direction, independently.
   c. The output of the previous item is the 3D real vector of the E field on each one of the simulated grid points in each direction. The physical implementation is that an ideal beam forming was done for the E field for each one of the points.
   d. The same process as described in item b is done for the H field.

$$\overrightarrow{H_{\text{UB},g}} = \vec{x}\sum_{k=1}^{N}\sqrt{\text{Re}[H_{kx,g}]^2 + \text{Im}[H_{kx,g}]^2} + \vec{y}\sum_{k=1}^{N}\sqrt{\text{Re}[H_{ky,g}]^2 + \text{Im}[H_{ky,g}]^2}$$
$$+ \vec{z}\sum_{k=1}^{N}\sqrt{\text{Re}[H_{kz,g}]^2 + \text{Im}[H_{kz,g}]^2} = \vec{x}\sum_{k=1}^{N}|H_{kx,g}| + \vec{y}\sum_{k=1}^{N}|H_{ky,g}| + \vec{z}\sum_{k=1}^{N}|H_{kz,g}|$$

   e. At each point in the grid, the Poynting vector is calculated by vector multiplication of the E and H fields, which are added up in items b and d. As explained before, without a loss of generality, we assume that the search plane is the x/y plane. All three (xyz) components of the Poynting vector are added, and not just the component that is normal to the x/y plane:

$$P_g = \frac{1}{2}Re\{(\vec{E} \times \vec{H}^*)\} = \frac{1}{2}Re\left\{\left(\left(E_yH_z^* - E_zH_y^*\right)\right)\hat{x} + \left(\left(E_zH_x^* - E_xH_z^*\right)\right)\hat{y} + \left(E_xH_y^* - E_yH_x^*\right)\hat{z}\right\}$$

$$P_{g,x} = \frac{1}{2}Re\{E_yH_z^* - E_zH_y^*\}$$

$$P_{g,y} = \frac{1}{2}Re\{(E_zH_x^* - E_xH_z^*)\}$$

$$P_{g,z} = \frac{1}{2}Re\{E_xH_y^* - E_yH_x^*\}$$

$$PUpperBound_g = \sqrt{P_{g,x}{}^2 + P_{g,y}{}^2 + P_{g,z}{}^2}$$

4. The above calculated Poynting vectors are used to estimate the power across 1cm^2 area.

$$P1cm2 = \iint_{1cm^2} PUpperBound_{g\;x,y,z}$$

5. The 1cm^2 area with the highest power value is used as the worst-case direction of a subset. The antenna phases are aligned to maximize the energy in this 1cm^2 area, as explained below in order to find the 2 worst cases:
    a. Turn on each element one-by-one to find order of power intensity in the 1cm^2 window. (Find the order of contribution)
    b. Sort in the power order from the highest to the lowest, #0 to #(10, 11, 11) for the involved subsets 1,2 and 3 respectively .
    c. Turn on #0 with phase P0=0. (reference)
    d. Turn on #1 and change the phase to maximize the power and find the phase P1.
    e. Keep P0 and P1 on, then turn on #2 and do same.
    f. Repeat for the rest of the antennas.
6. Using the antenna phases that were calculated in step 5, the power density is calculated along the evaluation plane and then spatially averaged across a 1cm^2 area.

A.1.5 3D models used in the simulation

A.1.5.1 Worst-case operating conditions of the platform

The Dell model T17G is a platform used in tablet mode. The worst case exposition to the radio frequency radiation can happen when the body of the user is in contact with the platform. The two evaluation planes illustrated Figure 12 represents the exposure planes according to subset radiation as mentioned in section A.1.4.

1. **Back-plane:** Is the evaluation plane for subset 1 and 3. In this case, the human body is below the tablet (blue area) – this mode represents the case in which a person holds the tablet and places it on their lap.

2. **Edge-plane:** Is the evaluation plane for subset 2. In this case, the human body is adjacent to platform edge (red area) – this mode represents the case in which a person is holding the tablet in their hand and the platform edge touching his body.
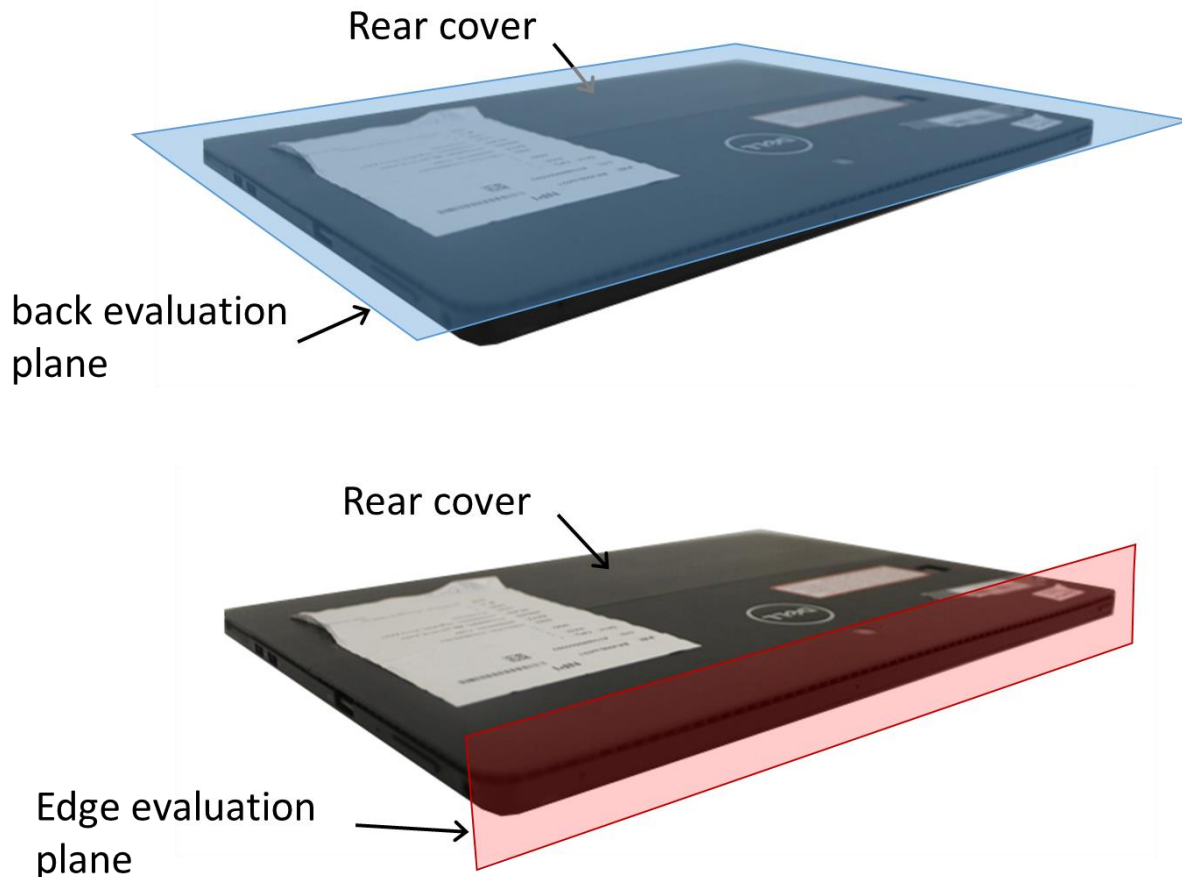
Figure 12 – Worst-case evaluation plane for Dell model T17G platform

A.1.5.2   RFEM 3 housing inside Intel 18265NGW module

The 3D Intel 18265NGW module is simulated inside the Dell T17G platform. Figure 13 shows the position of the RFEM 3 antenna, which is located inside the lid at the top left of the screen.
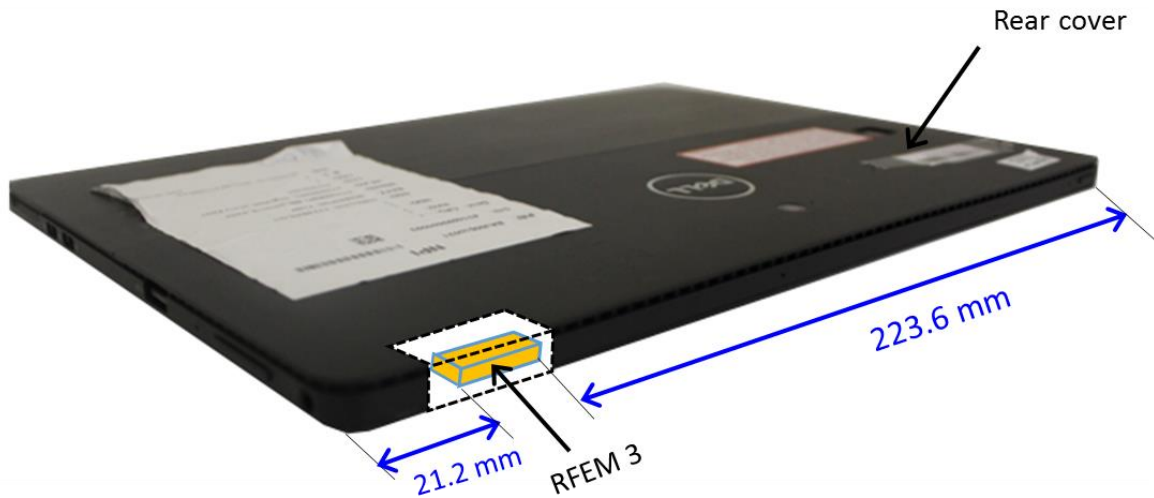
Figure 13 – Platform with RFEM 3 location

Intel

A.1.5.3 Closest distance to the body of an end user

In operating mode, the closest distance between the active antennas to the skin of an end user is when the person is holding the unit and touching the platform (at the evaluation plane) shown in Figure 12. In this case, two configuration were analyzed:

1. The human body is below the tablet – this mode represents the case in which a person places the tablet on their lap. In this scenario, the worst case emission is searched along the back evaluation plane (showed in blue in Figure 12) and the distance between human body to the active antenna is 1.49 mm.

2. The human body is adjacent to platform edge – this mode represents the case in which a person is holding the tablet in their hand and the tablet edge touching their body. In this scenario the worst case emission is searched along the edge plane (showed in red in Figure 12), in this case the distance between human body to the active antenna is 5.9 mm.

Figure 14 shows a cross-section (in the yz-plane) of the platform with the RFEM 3 inside the platform.
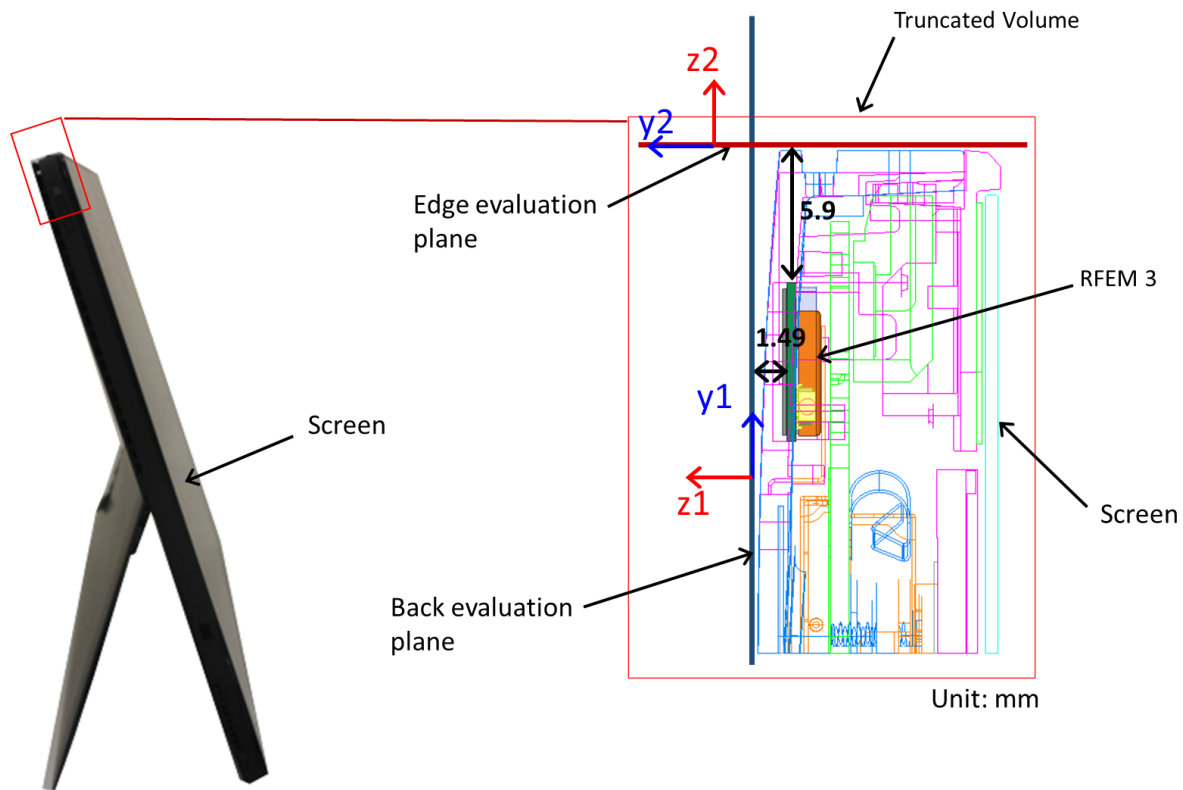
Figure 14 – Platform planes touching the body

A.1.5.4 Metals in proximity of the RFEM 3

All the metals that are in the RFEM 3 region (10 mm on each side) were included in the simulation.

A.1.6   Antenna feed

This section provides a general description of the numerical simulations; other details of the simulation geometry are included in reference [1]. The EM simulation uses an accurate 3D model of the RFEM 3 antenna. The model includes the antenna elements as well as their feeding lines.

In the simulation (as well as in the product), each antenna element is fed independently, and we excite the antennas at the origin of the antenna structure on the RFEM 3. (The antenna structure includes the silicon chip, the solder bumps, the vias, traces and actual antenna element.)

As described previously, the RFEM 3 antenna will be operated according to one of three predefined subsets. For the operational subset, signals of equal amplitude are applied to the feed-points of individual array elements, and the aggregate equivalent conducted power to all array elements *c*orresponds to the sum of all elements' powers. In the worst-case power density the subset 1 is the operational subset with an equivalent conducted power of 1.5 dBm; thus each element is fed by -8.5 dBm (1.5 dBm divided over ten elements).

The total power (same per element) is used to build the pattern of radiated power through beam forming. For building the beam forming pattern, the same power is used per element, while phase is changed per element. (Refer to Section 2.2 for more information about beam forming). Phases are derived for each excitation separately, to simulate the worst-case condition. Section A.1.4 explains how the phases are derived to find the worst case condition.

A.2 Power Density Simulation Results

A.2.1 Introduction

The evaluation planes presented in Section A.1.5.2 has been simulated according to the methodology described in Section A.1. The simulation results for all subsets in the concerned evaluation planes are presented in this section.

The power density has been simulated over three channels with frequencies listed in Table 5. For each channel, we'll present the resulting details according to the methodology explained in Section A.1.4:

- Simulation results of the upper bound single-point power density for each single-point across the mesh ($PUpperBound_g$). Please note that this value represents single-point power density and not spatially averaged power density over $1cm^2$. Even though a $1mW/cm^2$ scale is used, this value represents an upper-bound power density for each single point of the mesh, which is a much smaller area than $1cm^2$.

- The results of the single-point power density using the antenna phases corresponding to the first and second worst-cases.

- Spatially averaged power density over $1cm^2$ results of the first and second worst-case for each subset antenna phases. These results present the spatially averaged power density across $1cm^2$ using the xyz components of the Poynting vector.

Table 5 – WiGig channel frequencies

	Channel 1	Channel 2	Channel 3
Frequency (GHz)	58.32	60.48	62.64

Table 6 summarizes all the simulation configurations as well as the result types presented in this section:

Table 6 – Power density simulation configuration and result details

Subset	Evaluation Plane	Channels	Results types	Count	Reference
Subset 1	Back-plane	1, 2, and 3	Upper-bound power density	3 channels x 3 Subsets	Table 7
			1st worst-case antenna phases	3 channels x 3 Subsets	Table 8
Subset 2	Edge-plane		2nd worst-case antenna phases	3 channels x 3 Subsets	Table 9
			single point power density	2 Worst cases x 3 channels x 3 Subsets	Table 10
Subset 3	Back-plane		spatially averaged power density	2 Worst cases x 3 channels x 3 Subsets	Table 11
			Worst-case distribution[1]	[3 plots] – Very worst case	Section A.2.6

[1] The distribution of the found worst case spatially averaged power density among the 18 calculated worst cases.

A.2.2   Upper bound power density values in the evaluation plane

The Upper Bound single-point power density is calculated for each subset of the antenna.

Table 7 summarizes, for all subsets, the maximum calculated upper bound single point power density.

Please note that since the worst-case conditions are searched over a plane for near field, then the azimuth and the elevation are not relevant. The worst-case position is calculated using all the power density single-points issued from the upper-bound simulation results. We leverage the phase conditions for each antenna element that resulted in these worst-case conditions to evaluate final spatially averaged power density. The mathematical basis for using these as the worst-case phase conditions to evaluate the final spatially averaged power density is provided in Section A.1.4.3.

Table 7 – Maximum upper bound single point power density [mW/cm²]

	Channel 1	Channel 2	Channel 3
Subset 1	20.323	25.221	27.365
Subset 2	8.413	9.117	7.856
Subset 3	8.918	10.891	10.589

A.2.3   Worst-case antenna phases in the evaluation plane

The phase's configurations for the first and second worst power density cases are calculated for each subset and each channel using the phase search algorithm detailed in bullet 5 of Section A.1.4.3.

Table 8 and Table 9 shows, for each channel, the phases of each subset elements (marked in grey) in the first and second worst power density case respectively. The white cells with phase ("-") correspond to the non-active elements of the subset. For instance, for subset 1, the active elements are 7, 8; 17 to 24 and the worst case occurs for each channel with the indicated phases.

Note: The final antenna phases worst cases, used later in measurement, corresponds to the four highest maximum spatially averaged power density values among the eighteen calculated worst cases (3 channels x 3 subsets x 2 first worst-cases) showed in Table 11.

Table 8 –Phases configurations for the first worst case for all antenna subsets

Antenna index	Subset 1 – Back plane Phases [Degrees]			Subset 2 – Edge plane Phases [Degrees]			Subset 3 – Back plane Phases [Degrees]		
	CH1	CH2	CH3	CH1	CH2	CH3	CH1	CH2	CH3
1	-	-	-	-	-	-	90	270	90
2	-	-	-	-	-	-	270	90	270
3	-	-	-	-	-	-	90	90	270
4	-	-	-	0	0	0	-	-	-
5	-	-	-	0	0	0	-	-	-
6	-	-	-	270	270	270	-	-	-
7	0	90	0	-	-	-	-	-	-
8	270	270	270	-	-	-	-	-	-
9	-	-	-	180	270	90	-	-	-
10	-	-	-	270	0	90	-	-	-
11	-	-	-	270	90	0	-	-	-
12	-	-	-	0	90	90	-	-	-
13	-	-	-	0	90	90	270	270	180
14	-	-	-	90	180	180	0	0	0
15	-	-	-	90	270	180	270	270	270
16	-	-	-	180	90	270	0	90	0
17	0	0	0	-	-	-	-	-	-
18	180	180	180	-	-	-	-	-	-
19	90	0	0	-	-	-	-	-	-
20	270	180	180	-	-	-	-	-	-
21	270	270	0	-	-	-	180	180	0
22	270	270	0	-	-	-	0	180	0
23	270	270	270	-	-	-	180	270	90
24	270	90	180	-	-	-	180	270	90

Table 9 –Phases configurations for the second worst case for all antenna subsets

Antenna index	Subset 1 – Back plane Phases [Degrees]			Subset 2 – Edge plane Phases [Degrees]			Subset 3 – Back plane Phases [Degrees]		
	CH1	CH2	CH3	CH1	CH2	CH3	CH1	CH2	CH3
1	-	-	-	-	-	-	90	270	0
2	-	-	-	-	-	-	270	90	180
3	-	-	-	-	-	-	180	90	180
4	-	-	-	0	0	0	-	-	-
5	-	-	-	0	0	0	-	-	-
6	-	-	-	180	0	0	-	-	-
7	270	180	270	-	-	-	-	-	-
8	180	90	180	-	-	-	-	-	-
9	-	-	-	0	270	90	-	-	-
10	-	-	-	180	0	90	-	-	-
11	-	-	-	90	90	0	-	-	-
12	-	-	-	270	0	00	-	-	-
13	-	-	-	0	90	180	180	0	270
14	-	-	-	180	180	0	0	0	0
15	-	-	-	0	0	180	180	0	270
16	-	-	-	0	90	270	270	90	90
17	0	0	0		-	-	-	-	-
18	180	90	90		-	-	-	-	-
19	90	90	0	-	-	-	-	-	-
20	270	270	180	-	-	-	-	-	-
21	270	180	270	-	-	-	90	270	270
22	180	90	180	-	-	-	270	90	90
23	180	90	180	-	-	-	90	270	180
24	270	270	0	-	-	-	90	270	180

A.2.4   Single-Point power density values in the evaluation plane

Table 10 presents, for all channels and subsets, the calculated single-point power density values in the concerned evaluation plane using the first and the second worst-case subset antenna phases presented in Table 8 and Table 9 respectively.

Table 10 – Maximum single point power density [mW/cm^2]

	First worst case			Second worst case		
	Channel 1	Channel 2	Channel 3	Channel 1	Channel 2	Channel 3
Subset 1	3.222	3.708	3.890	3.197	4.434	3.983
Subset 2	1.127	0.484	0.465	1.363	0.367	0.431
Subset 3	1.616	2.826	2.895	1.859	2.316	2.770

A.2.5 Spatially averaged power density over 1 cm^2 values in the evaluation plane

Table 11 shows, for all channels and subsets, the calculated spatially averaged power density over 1 cm^2 at 100% duty cycle. These values are calculated in the concerned evaluation plane using the first and the second worst-case subset antenna phases shown in Table 8 and Table 9 respectively.

Table 11 – Maximum spatially averaged power density over 1cm^2 [mW/cm^2]

	First worst case			Second worst case		
	Channel 1	Channel 2	Channel 3	Channel 1	Channel 2	Channel 3
Subset 1	0.845	**0.907**	0.867	0.803	0.836	0.808
Subset 2	0.183	0.178	0.149	0.166	0.088	0.118
Subset 3	0.608	0.602	0.589	0.564	0.568	0.570

Table 11 shows that the worst case is found for **subset 1 at channel 2** with spatially averaged power density of **0.907 mW/cm^2** at 100 % duty cycle. The next section presents all power density distributions for this worst cases.

A.2.6 Worst case power density distribution

As described in the previous section, the worst case spatially averaged power density over 1 cm^2 among the eighteen calculated worst-cases is found for subset 1, channel 2. The worst case subset antenna phase's configuration used in this case is for the first worst case (see Table 8, subset 1 / channel 2 configuration).

This section present for this worst case the distribution of the following listed items:

- Upper bound single point power density distribution
- Single-point power density distribution
- One dimensional cut of the single-point power density distribution
- Spatially averaged power density over 1 cm^2

A.2.6.1 Upper-bound power density distribution

Figure 15 presents upper-bound, single-point power density of subset 1, channel 2 which is the worst case among the two simulated worst cases of the three subsets. The evaluation plane of subset 1 is the back-plane represented in Figure 12.

The footprint of the platform components in the back evaluation plane for single-point power density representation is shown in Figure 17.

Worst-case coordinates on channel 2 are X=-0.100 cm, Y=0.030 cm.

Figure 15 – Channel 2 upper-bound, single-point power density

A.2.6.2   Single point power density distribution

Figure 16 presents the single-point power density distribution of subset 1, channel 2 in the back-plane using the worst-case antenna phases of subset 1, channel 2 (see Table 8)

The footprint of the platform components in the back plane for single-point power density representation is shown in Figure 17.

Worst-case coordinates on channel 2 are X=-0.2900 cm, Y=0.04000 cm.

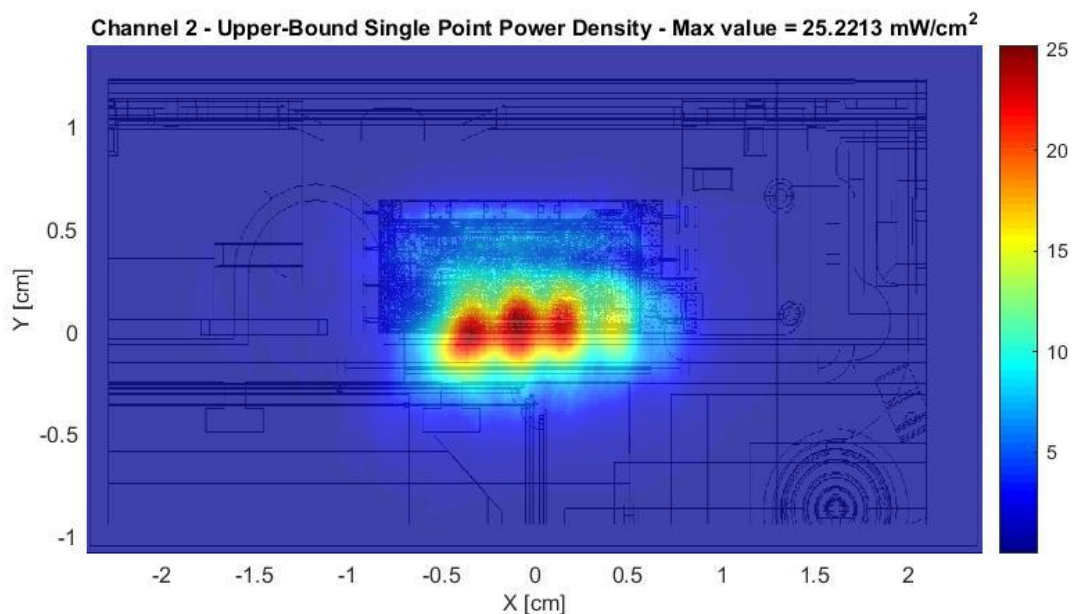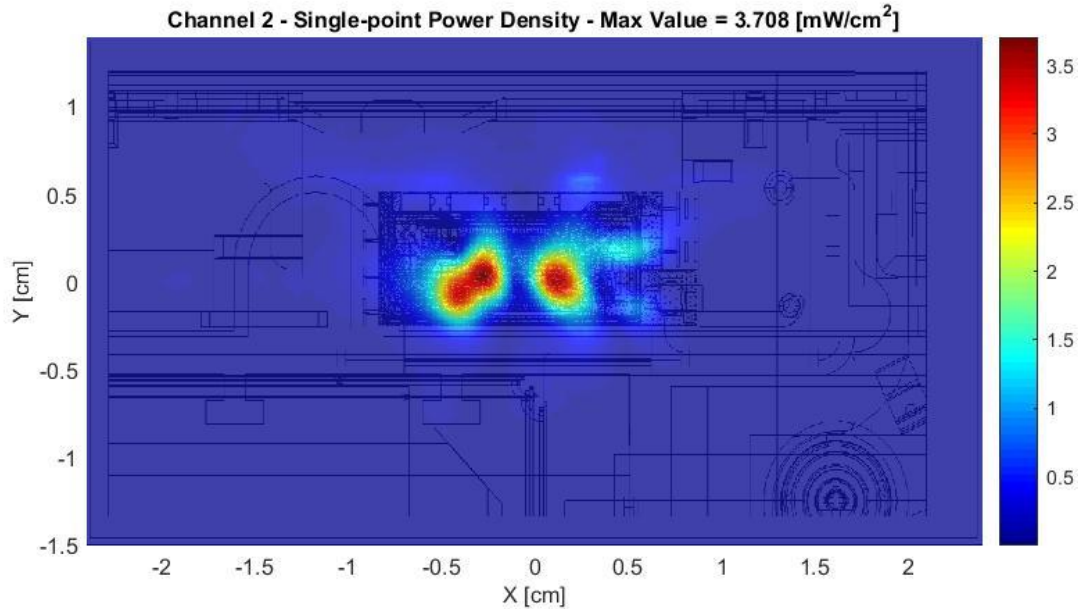**Figure 16 – Channel 2 single-point power density**
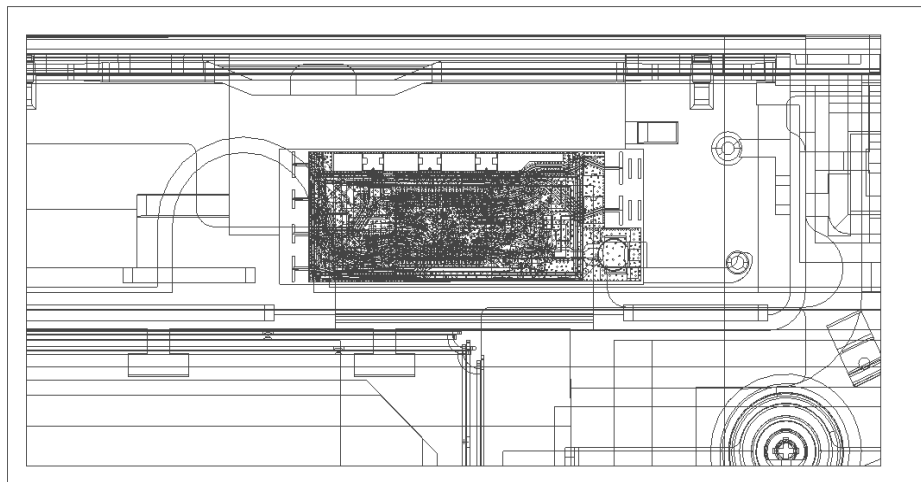
Figure 17 – Footprint of single-point power density plane representation

A.2.6.3 One dimensional cut of the single-point power density distribution

In Figure 18 and Figure 19, we present the simulation results from the xyz components of single-point power density values with worst-case antenna phases of subset 1, channel 2 which is the worst case among the three subsets. The figures represent a 1-dimensional cut in the x-axis and y-axis that shows the behavior of the near field power density at the evaluation plane.

Channel 2 - 1D Power Density [mW/cm^2] along X dimension
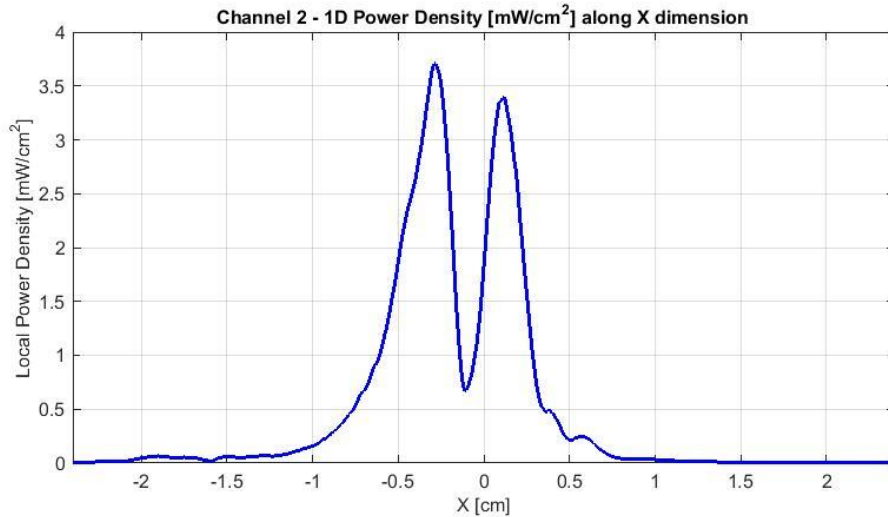
Figure 18 – 1-dimensional plots of the power density along x dimension

Channel 2 - 1D Power Density [mW/cm^2] along Y dimension

Figure 19 – 1-dimensional plots of the power density along y dimension

A.2.6.4 Distribution of Spatially averaged power density over 1 cm^2

Figure 20 presents the spatially averaged power over 1cm^2 at 100% duty cycle for the worst-case scenario of subset 1, channel 2 as explained in Section A.1.4.3.

The 1cm^2 square location correspondent to the maximum of spatially averaged power density value is plotted in Figure 20 for the channel 2.

Worst-case coordinates on channel 2 are X=-0.1300 cm, Y=0.13000 cm.
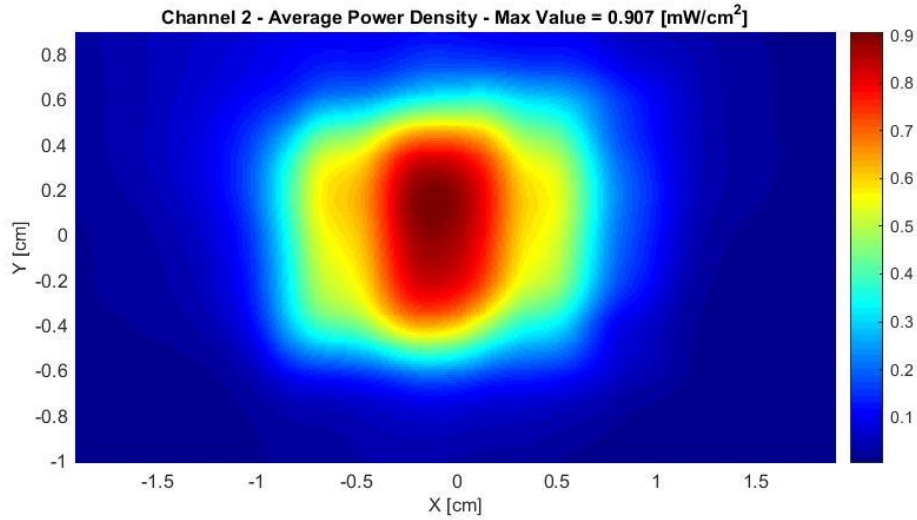
Figure 20 – Channel 2– spatially averaged power density over 1cm^2
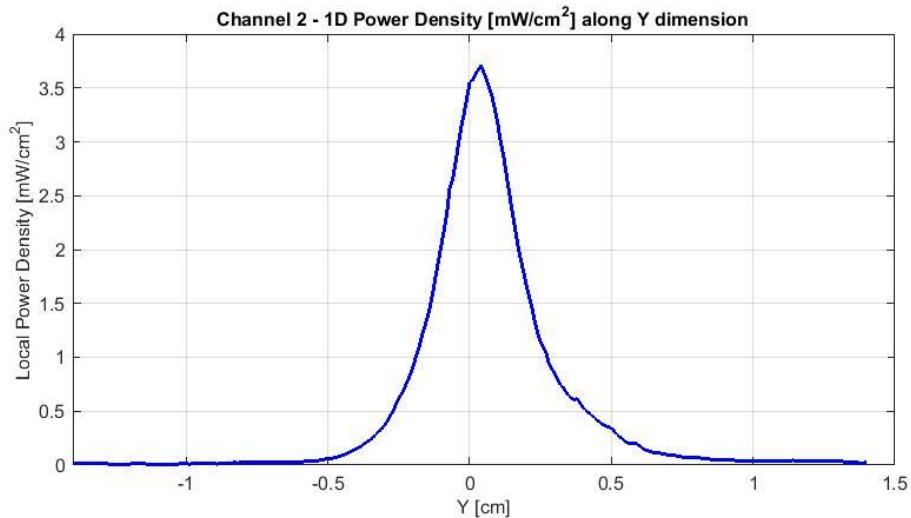
The Table 12 shows the simulated worst-case power density, for subset 1 – channel 2, in the evaluation plane.

Table 12 – Worst-case power density

Highest power density	Subset 1 - Channel 2
70% duty cycle	0.635
100% duty cycle	0.907

Notes for Table 12

1. The worst-case power density is found for channel 2 on subset 1.

2. The Maximum power density (spatially averaged over worst 1cm^2) in channel 2 is achieved at 0 mm distance from the platform boundary and equals 0.907 mW/cm^2 over 100% duty cycle.

3. As explained in Section 2.4, the Intel 18265NGW module is limited to transmit at a duty cycle of 70% over 10 seconds. Therefore the maximum spatially-integrated and time-averaged power density over 1cm^2 is 0.907 x 0.7 = 0.635 mW/cm^2.

A.2.7   Conclusion

The simulation results for the three subsets in the concerned evaluation plane for three channels were presented in this report. The worst case is observed on channel 2 for subset 1, with the maximum total spatially averaged power density of 0.635 mW/cm^2. Note that the applicable FCC limit is 1 mW/cm^2.

Appendix B: Supplemental Validation of RF Exposure Power Density Simulations Using Near-Field Measurements

B.1 Introduction

In this section, the near field power density measurement performed using the worst case antenna phases found by simulation is presented. This near field measurement provides the validation of the simulation presented in Section A.2. Indeed, because the measurement results are unavailable at distances closer than 2 mm, the comparison between simulation and measurement is performed at 2 mm and 5 mm from the evaluation plane.

A near-field RF exposure system from SPEAG is used to perform these measurements.

B.2 Probe Characteristics

The probe consist of two dipoles (0.8 mm length) optimally arranged with different angles (γ1 and γ2) to obtain pseudo-vector information, printed on glass substrate protected by high density foam that allows low perturbation of the measured field.

Three or more measurements are taken for different probe rotational angles, deriving the amplitude and polarization information.

The probe's characteristics are illustrated in Table 13

Table 13 – Near Field probe Characteristics

Frequency Range	750 MHz – 110 GHz[3]
Length	320 mm
Probe tip external diameter	8 mm
Distance between diode sensors and probe's tip	1.5 mm
Axial Isotropy	±0.6 dB
Maximum operating E-field	3000 V/m
Lower E-field detection threshold	5 V/m @ 60 GHz

More details about the measurement system are found in reference [2].

---

[3] *The probe calibration range is 750 MHz – 90 GHz*

B.3 Total Field and Power Flux Density Reconstruction

Computation of the power density in general requires knowledge of the electric (E-) and magnetic (H-) field amplitudes and phases in the plane of incidence. Reconstruction of these quantities from pseudo-vector E-field measurements is feasible, as they are constrained by Maxwell's equations.

The reconstruction algorithm developed by the system manufacturer, together with the ability of the probe to measure extremely close to the source without perturbing the field, permits reconstruction of the E- and H-fields, as well as of the power density, on measurement planes located as near as 0.4λ away.

The average of the reconstructed power density is evaluated over a circular area in each measurement plane. The area of the circle is defined by the user; the default is 1 cm^2.

B.4 Measurement configurations

The near field measurement is performed on the four highest maximum spatially averaged power density found among the eighteen calculated worst cases (3 channels x 3 subsets x 2 first worst-cases) showed in Table 11. The test configurations are summarized in Table 14.

Table 14 – Test Configuration

Measurement Configuration			
EUT	Dell Model T17G		
Measured cases	Four highest worst cases* found in simulation:		
		Subset	**Channel**	**Worst-case**
	Case 1#	1	2	1
	Case 2#	1	2	2
	Case 3#	3	1	1
	Case 4#	3	3	2
Measurement Distances / Resolution / Scan Plane		**Distance**	**Scan Plane size [cm^2]**	**Resolution [mm]**
	Case 1#	2 mm / 5 mm	3.84x3.84 / 4.34x4.34	1.2
	Case 2#	2 mm / 5 mm	4.34x4.34	1.2
	Case 3#	2 mm / 5 mm	4.24x4.24	1.3
	Case 4#	2 mm / 5 mm	4.43x4.43 / 3.71x3.71	1.2

* The phases' combination is that showed in Table 8 and Table 9.

B.5 Measurement results

Tables 15 through 18 show the comparison between simulation and measurement for the four measured worst-cases at 2 and 5 mm distances from the evaluation plane. All results are calculated at 100 % duty cycle.

Table 15 – Case 1#: Simulation Vs. test results @ 2 and 5 mm.

	Measurement Distance (mm)	Simulated	Measured	Max. Deviation (dB)
E-field (V/m)	2 mm	129.271	118.033	0.790
	5 mm	86.419	76.030	1.113
H-field (A/m)	2 mm	0.344	0.399	1.290
	5 mm	0.230	0.287	1.937
Single-point PD (mW/cm²)	2 mm	2.147	2.124	0.047
	5 mm	1.040	0.826	1.003
Average PD (mW/cm²)	2 mm	0.620	0.494	0.980
	5 mm	0.382	0.269	1.513

Table 16 – Case 2#: Simulation Vs. test results @ 2 and 5 mm.

	Measurement Distance (mm)	Simulated	Measured	Max. Deviation (dB)
E-field (V/m)	2 mm	127.862	164.932	2.211
	5 mm	88.266	101.861	1.244
H-field (A/m)	2 mm	0.337	0.348	0.272
	5 mm	0.260	0.311	1.562
Single-point PD (mW/cm²)	2 mm	2.134	2.827	1.222
	5 mm	1.166	1.449	0.943
Average PD (mW/cm²)	2 mm	0.679	0.802	0.723
	5 mm	127.862	164.932	2.211

Table 17 – Case 3#: Simulation Vs. test results @ 2 and 5 mm.

	Measurement Distance (mm)	Simulated	Measured	Max. Deviation (dB)
E-field (V/m)	2 mm	82.244	104.925	2.115
	5 mm	55.182	73.898	2.537
H-field (A/m)	2 mm	0.229	0.215	0.572
	5 mm	0.161	0.226	2.945
Single-point PD (mW/cm²)	2 mm	0.813	1.118	1.382
	5 mm	0.432	0.684	2.000
Average PD (mW/cm²)	2 mm	0.311	0.241	1.117
	5 mm	0.176	0.253	1.576

Table 18 – Case 4#: Simulation Vs. test results @ 2 and 5 mm.

	Measurement Distance (mm)	Simulated	Measured	Max. Deviation (dB)
E-field (V/m)	2 mm	115.030	95.662	1.601
	5 mm	63.355	80.050	2.032
H-field (A/m)	2 mm	0.275	0.216	2.071
	5 mm	0.172	0.211	1.756
Single-point PD (mW/cm²)	2 mm	1.552	0.989	1.959
	5 mm	0.594	0.706	0.749
Average PD (mW/cm²)	2 mm	0.358	0.275	1.151
	5 mm	0.225	0.250	0.454

Figures below show the comparison at 2 mm and 5 mm from the evaluation plane, between the simulation and the near field measurement in terms of E-Field, H-Field, Single-point Power Density and Spatially Averaged Power Density at 100 % duty cycle for the four higher worst cases.

Note that the fields results presented in the figures below consider a peak phasor for electromagnetic fields **for both simulation and measurement.**

Case #1 - DISTANCE = 2 mm

Simulated	Measured

E-field - Max Value = 129.271 [V/m]

E-field - Max Value = 118.033 [V/m]

E-field (V/m) @ 2 mm – Deviation of Max Value: 0.790 dB

H-field - Max Value = 0.344 [A/m]

H-field - Max Value = 0.399 [A/m]

H-field (V/m) @ 2 mm – Deviation of Max Value: 1.290 dB

Single-point PD - Max Value = 2.147 [mW/cm^2]

Single-point PD - Max Value = 2.124 [mW/cm^2]

Localized free space PD (mW/cm2) @ 2 mm – Deviation of Max Value: 0.047 dB

Average PD - Max Value = 0.620 [mW/cm^2]

Average PD - Max Value = 0.494 [mW/cm^2]

Spatially Averaged PD (mW/cm2) @ 2 mm – Deviation of Max Value: 0.980 dB

Case #1 - DISTANCE = 5 mm

Simulated	Measured

E-field (V/m) @ 5 mm – Deviation of Max Value: 1.113 dB

H-field (V/m) @ 5 mm – Deviation of Max Value: 1.937 dB

Localized free space PD (mW/cm2) @ 5 mm – Deviation of Max Value: 1.003 dB

Spatially Averaged PD (mW/cm2) @ 5 mm – Deviation of Max Value: 1.513 dB

Case #2 - DISTANCE = 2 mm

Simulated	Measured

E-field - Max Value = 127.862 [V/m]

E-field - Max Value = 164.932 [V/m]

E-field (V/m) @ 2 mm – Deviation of Max Value: 2.211 dB

H-field - Max Value = 0.337 [A/m]

H-field - Max Value = 0.348 [A/m]

H-field (V/m) @ 2 mm – Deviation of Max Value: 0.272 dB

Single-point PD - Max Value = 2.134 [mW/cm^2]

Single-point PD - Max Value = 2.827 [mW/cm^2]

Localized free space PD (mW/cm2) @ 2 mm – Deviation of Max Value: 1.222 dB

Average PD - Max Value = 0.679 [mW/cm^2]

Average PD - Max Value = 0.802 [mW/cm^2]

Spatially Averaged PD (mW/cm2) @ 2 mm – Deviation of Max Value: 0.723 dB

Intel

Case #2 - DISTANCE = 5 mm

Simulated	Measured

E-field (V/m) @ 5 mm – Deviation of Max Value: 1.244 dB

H-field (V/m) @ 5 mm – Deviation of Max Value: 1.562 dB

Localized free space PD (mW/cm2) @ 5 mm – Deviation of Max Value: 0.943 dB

Spatially Averaged PD (mW/cm2) @ 5 mm – Deviation of Max Value: 0.613 dB

Case #3 - DISTANCE = 2 mm	
Simulated	**Measured**

E-field (V/m) @ 2 mm – Deviation of Max Value: 2.115 dB

H-field (V/m) @ 2 mm – Deviation of Max Value: 0.572 dB

Localized free space PD (mW/cm2) @ 2 mm – Deviation of Max Value: 1.382 dB

Spatially Averaged PD (mW/cm2) @ 2 mm – Deviation of Max Value: 1.117 dB

Case #3 - DISTANCE = 5 mm	
Simulated	**Measured**
E-field - Max Value = 55.182 [V/m]	E-field - Max Value = 73.898 [V/m]
E-field (V/m) @ 5 mm – Deviation of Max Value: 2.537 dB	
H-field - Max Value = 0.161 [A/m]	H-field - Max Value = 0.226 [A/m]
H-field (V/m) @ 5 mm – Deviation of Max Value: 2.945 dB	
Single-point PD - Max Value = 0.432 [mW/cm^2]	Single-point PD - Max Value = 0.684 [mW/cm^2]
Localized free space PD (mW/cm2) @ 5 mm – Deviation of Max Value: 2.000 dB	
Average PD - Max Value = 0.176 [mW/cm^2]	Average PD - Max Value = 0.253 [mW/cm^2]
Spatially Averaged PD (mW/cm2) @ 5 mm – Deviation of Max Value: 1.576 dB	

Case #4 - DISTANCE = 2 mm

Simulated	Measured

E-field - Max Value = 115.030 [V/m]

E-field - Max Value = 95.662 [V/m]

E-field (V/m) @ 2 mm – Deviation of Max Value: 1.601 dB

H-field - Max Value = 0.275 [A/m]

H-field - Max Value = 0.216 [A/m]

H-field (V/m) @ 2 mm – Deviation of Max Value: 2.071 dB

Single-point PD - Max Value = 1.552 [mW/cm^2]

Single-point PD - Max Value = 0.989 [mW/cm^2]

Localized free space PD (mW/cm2) @ 2 mm – Deviation of Max Value: 1.959 dB

Average PD - Max Value = 0.358 [mW/cm^2]

Average PD - Max Value = 0.275 [mW/cm^2]

Spatially Averaged PD (mW/cm2) @ 2 mm – Deviation of Max Value: 1.151 dB

Case #4 - DISTANCE = 5 mm

Simulated	Measured

E-field (V/m) @ 5 mm – Deviation of Max Value: 2.032 dB

H-field (V/m) @ 5 mm – Deviation of Max Value: 1.756 dB

Localized free space PD (mW/cm2) @ 5 mm – Deviation of Max Value: 0.749 dB

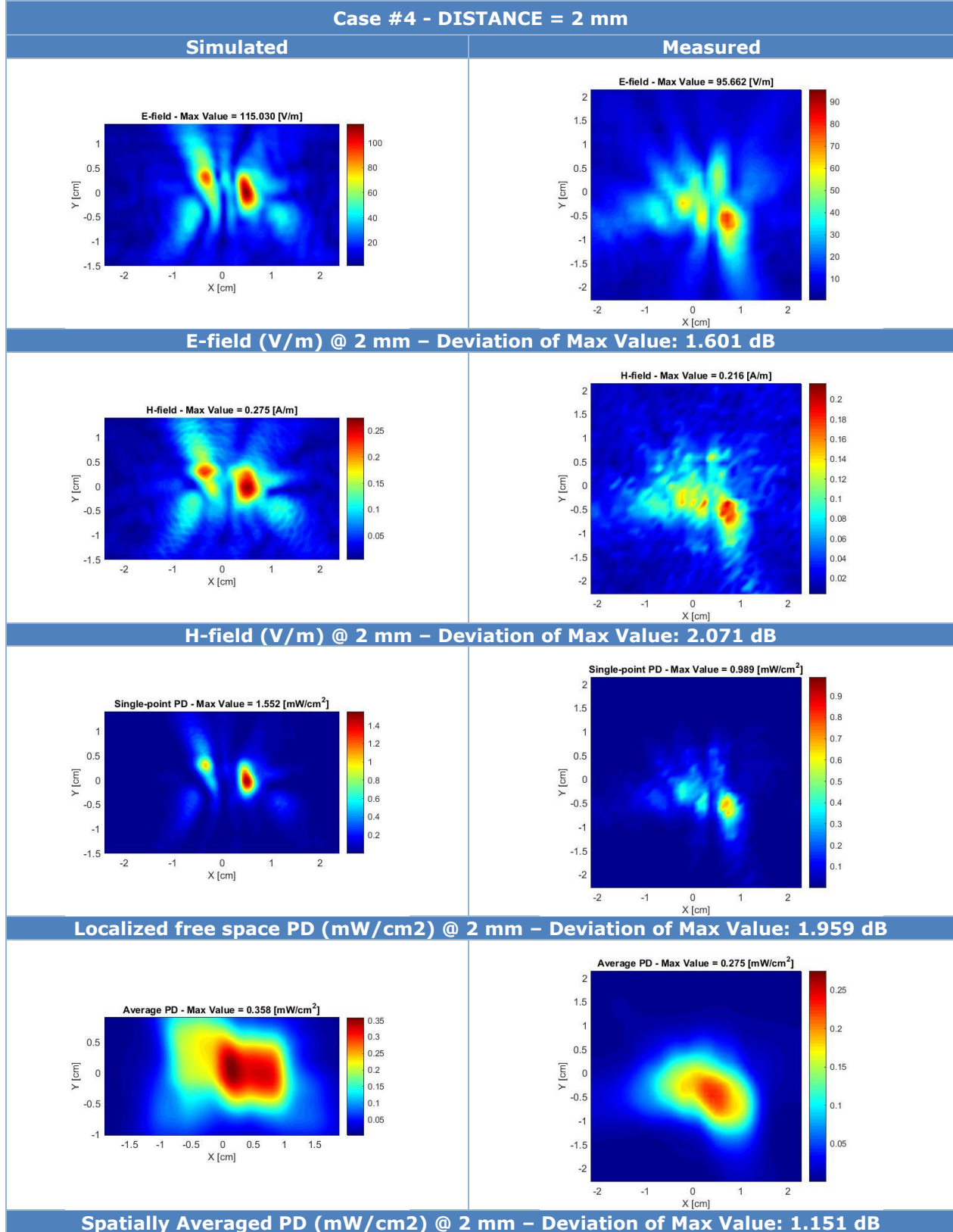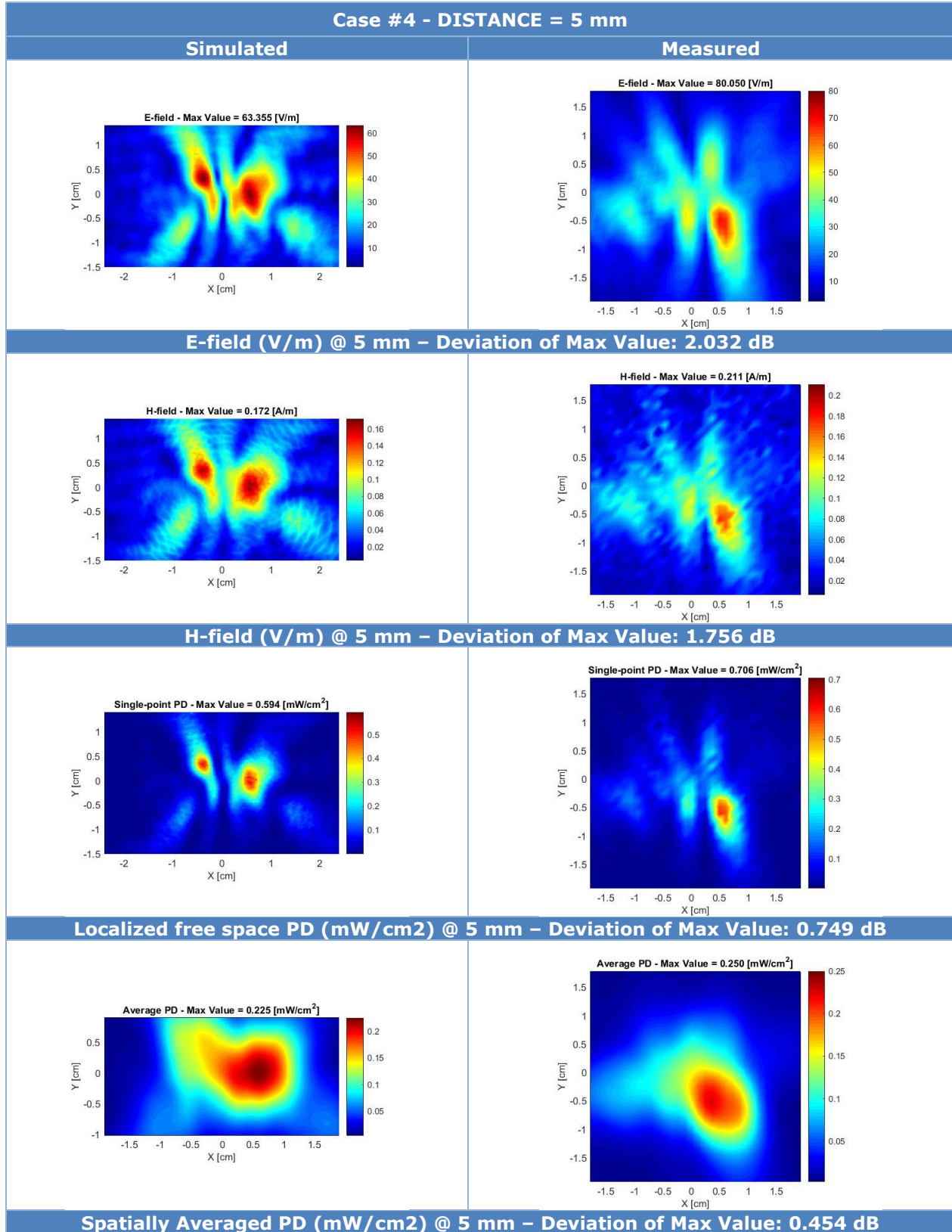### Spatially Averaged PD (mW/cm2) @ 5 mm – Deviation of Max Value: 0.454 dB

B.6 Conclusion

The near field measurement shows a good correlation with the near field simulation with a maximum deviation below 3 dB for the measured distances. This correlation is considered as a validation of the simulation process and the resulting worst case